

الجمهورية الجزائرية الديمقراطية الشعبية
وزارة التعليم العالي والبحث العلمي

Universite Badji Mokhtar - Annaba
Badji Mokhtar – Annaba University



جامعة باجي مختار – عنابة

Faculty: Technology
Department: Electrical engineering
Domain: electrical engineering
Function: Computer science
Specialty: [Electric Control]

Theme

Modeling and Optimization of a Photovoltaic System for Supplying a Dewater Rural Station

Represented by : Bouatba meriem

Supervisor : Dr GHOUELBOURLK Sihem

Grade MCA

University

Examining committee :

Hadjabi mohamed	Grade Pr	University	President
GHOUELBOURLK Sihem	Grade MCA	University	Supervisor
Chelli Seif Elislem	Grade MCB	University	Examineur

College year : 2023/2024

Thanking

First of all, praise to «ALLAH» who guided us on the right path throughout the work and inspired us to do the good and the right reflexes. Without his mercy, this work will not be successful.

We would like to express our thanks and gratitude to D^r. Ghoudelbourlk Sihem for all her efforts; her moral and scientific support allowed us to complete this labor.

Our sincere thanks also go to the members of the jury who have agreed to evaluate this work.

My sincere thanks also go to all the teachers of the electrical engineering department of the university, Badji Mokhtare Annaba, for the training that they provided.

have ensured throughout our university curriculum and to all those to whom we owe our training.

Finally, we would like to thank all our colleagues and our friends for their moral support and to all those who participated to some extent in the development of this work.



Dedicace

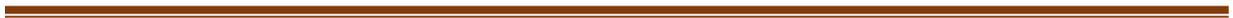
الحمد لله رب العالمين تبارك و تعالى له الكمال وحده و الصلاة و السلام على سيدنا محمد و رسوله الأمين و على سائر الأنبياء المرسلين احمد الله تعالى الذي بارك لي في إتمام بحثي هذا و أتقدم بجزيل الشكر و الامتنان

الى من كلله المولى بالهيبة و الوقار الى من احمل اسمه بكل افتخار ابي رحمه الله * سعيد *
الى القلب النابض و رمز الحنان و القوة ابي * غنية بوهيمة *
الى نفسي التي صبرت و اجتهدت الى ان حققت
الى السند الدائم الذي لا يميل اخوتي * كريمة * سومية * محمد * ايمان *
الى اميراتي * رزان * هزار *

الى من احسنوا بي الظن و رؤوا فيا الخير باعينهم و قلوبهم الى جميع المؤسسات التطوعية التي صنعت شخصيتي و ساهمت في بروزها و تكوينها و الى أصدقاء الرحلة الذين كانوا سحبا ممطرا الى ارض النضال و الأمل الى الأجل منا الصامدين على ثغورهم الى غزة العزة و القدس الشريف و فلسطيننا الالية و شهدائها الابرار

- واعلموا انا مهمتكم ليست شهادة تناولها و لكن مهمتكم امة تحيينها -

Summary



Summary

General introduction	1
-----------------------------------	---

Chaptre I : Photovoltaic pumping system

I.1 Introduction.....	2
I.2 Photovoltaic pumping system.....	3
I.2.1 Pumping over sun	3
I.2.2 Pumping with electrochemical storage (batteries)	3
I.3 The photovoltaic system	4
I.3.1 Photovoltaic effect	4
I.3.1.1 The photovoltaic cell.....	4
I.3.2 The principle of operation	5
I.3.2.1 The deferent types of photovoltaic cell.....	5
I.3.3 The photovoltaic module	6
I.3.4 Different types of photovoltaic system.....	7
I.3.4.1 Phtovoltaic systems connected to the grid	7
I.3.4.2 Autonomous photovoltaic system.....	8
I.3.4.2.1 Autonomous systems without electrochemical storage	8
I.3.4.2.2 Stand-alone systems with electrochemical storage	8
I.4 Solar energy in Algeria	8
I.5 Photovoltaic generator	9
I.6 Static converters used in photovoltaic pumping systems	10
I.6.1 DC/DC converter (chopper)	10
I.6.1.1. Buck converter (series chopper)	10
I.6.1.2 Boost converter (parallel chopper)	10
I.6.1.3 DC/AC converter (inverter)	11
I.7 Motors-pump unit	11
I.7.1 Motors (IM machine)	11
I.7.2 The pumps	11
I.7.2.1 Types of pumps.....	12
I.7.3 The centrifugal pump.....	12
I.8 Conclusion	12

Chapter II : Modelling of photovoltaic pumping system

II.1 Introduction	13
II.2 Photovoltaic solar energy	13
II.2.1 Modelling of the power system.....	15
II.2.2 Modelling of the photovoltaic generator	15
II.2.3 Electrical modelling of a photovoltaic cell.....	16
II.2.4 Parameters of a photovoltaic cell	17
II.2.4.1 Shorts circuit current (I_{cc})	17

II.2.4.2 Open circuit voltage (V_{co})	17
II.2.5 Advantages and disadvantages of PV system.....	18
II.3 The static converters	18
II.3.1 Boost choper	19
II.3.2 Operation of boost choper	20
II.3.3 Mathematical model equivalents	20
II.4 Principle of operation of in inverter	21
II.4.1 Three-phase inverter	22
II.5 Inverter modelling	23
II.5.1 Voltage inverter model	23
II.6 MI motors modelling	25
II.6.1 Dynamic modelling	25
II.6.1.1 Advantages of the IM.....	25
II.6.1.2 IM problem	25
II.6.2 Simplifying assumptions	26
II.6.3 IM speed selector	28
II.6.4 Equation of the IM.....	28
II.7 Centrifugal pumps.....	31
II.7.1 Using of centrifuge pumps.....	31
II.7.2 Operation of centrifuge pumps.....	32
II.7.3 The mathematical model of centrifugal pump.....	32
II.7.3.1 Hydraulic model.....	32
II.7.3.2 Mechanical model.....	33
II.8 Conclusion	34

Chapter III : Desing and simulation of the photovoltaic pumping system

III.1 Introduction	31
III.2 Sizing of a photovoltaic pumping system	31
III.2.1 Sizing of the photovoltaic field	31
III.2.1.1 Determination of available solar energy.....	31
III.2.2 Engine sizing	33
III.2.3 Dimensioning of the centrifugal pump.....	33
III.3 Definition of direct torque control technology DTC	33
III.3.1 Principle of DTC.....	34
III.3.2 Flow and torque control	34
III.3.2.1 Flow control.....	35
III.3.2.2 Torque control	35
III.3.3 DTC stratgy.....	36
III.3.4 Estimators.....	36
III.3.4.1 Stator flow estimates	36
III.3.4.2 Estimators of electromagnetic cutting	37
III.3.5Correctors	37
III.3.5.1 Flow corrector	37
III.3.5.2 Torque corrector.....	38
III.3.6 Choice of voltage vector.....	38

III.3.7 Elaboration of the switching tables	39
III.3.7.1 Switch table with null sequences	39
III.3.7.2 Switch table with aout null sequences.....	40
III.3.8 The advantages and disadvantages	41
III.4. The MPPT command	42
III.4.1 The main features and functionality	43
III.4.2 The methods of the MPPT command	43
III.4.3 The perturbation and observation method.....	43
III.5 Simulation and results.....	44
III.6 Conclusion.....	47
General conclusion.....	48



List of figurs



Chapter I: Photovoltaic pumping system

Fig I.1 Solar livestock pumping systems and water irrigation.....	2
Fig I.2 Conversion steps.....	2
Fig I.3 Working principle of pumping to the sun wire.....	3
Fig I.4 Photovoltaic pumping with energy storage	4
Fig I.5 Principle of operation of a photovoltaic cell	5
Fig I.6 Characteristic current voltage N_s cell in series.....	6
Fig I.7 Characteristic current voltage of (N_p) cells in parallel.....	6
Fig I.8 Photovoltaic system connected to the grid	7
Fig I.9 Preliminary map of solar irradiations in Algeria	8
Fig I.10 Components of a photovoltaic module generator.....	9
Fig I.11 The schematic of the series chopper.....	10
Fig I.12 The schematic of the parallel chopper	10
Fig I.13 View in front of a centrifugal pump	11
Fig I.14 Example of installation with a centrifugal pump.....	12

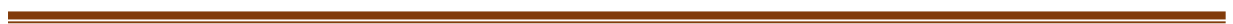
Chapter II: Modelling of photovoltaic pumping system

Fig II.1 photovoltaic system.....	13
Fig II.2 Modelling of the equivalent electrical circuit of a PV cell [20].....	14
Fig II.3 Equivalent scheme of a photovoltaic cell under illumination	16
Fig II.4 the different types of static converters.	18
Fig II.5 Electrical diagram of a boost chopper.....	18
Fig II.6 Chronograms of current and voltage of a boost chopper	19
Fig II.7 Electrical diagram of a closed boost chopper.....	19
Fig II.8 Electrical diagram of an open boost chopper	20
Fig II.9 inverter operation diagram	20
Fig II.10 Schematic diagram of a three-phase bridge inverter.....	21
Fig II.11 simplified model of the three-phase inverter	21
Fig II.12 Induction motor	23
Fig II.13 stator schema	24
Fig II.14 centrifugal pump	28
Fig II.15 Working principle of centrifugal pump.....	29

Chapter III: Design and simulation of the photovoltaic pumping system

Fig I.1 DTC structure diagram applied to an IM.....	33
Fig I.2 Evolution of the flux vector in the $\alpha\beta$ plane	33
Fig I.3 DTC control block diagram	35
Fig I.4 starting from the complex plane in six sectors	39
Fig I.5 Solar power conversion chain including MMPT control	400
Fig III.6 Block diagram of the P&O method.	422
Fig III.7 Perturbation and observation method algorithm.....	433
Fig III.8 Reven of variation of current i and power as a function of time	444
Fig III.9 Reven of variation of current and power as a function of time	444
Fig III.10 Reven of variation of current and power as a function of time.....	455

Fig III.11 Reven of variation of hydrolic power as a function of time	Erreur ! Signet non défini.5
Fig III.12 Reven of variation of torque as a function of time	455
Fig III.13 Reven of variation of speed as a function of time	46
Fig III.14 Reven of variation of empty corrant as a function of time.....	46



Tables list



Tables

Chapter I: Photovoltaic pumping system

Table I.1 Solar energy potential in Algeria.....	8
--	---

Chapter III: Desing and simulation of the photovoltaic pumping system

Table III.1 Table for the choice of tension vectors.	38
Table III.2 Switching table defined by Takahachi.....	39
Table III.3 PV module parametre	44

Notions and abreviation



Notions

I : the current delivered by the module
I_d : diode current
I_{sat} : saturation current
I_{ch} : the current of the shunt resistor
T_a : ambient temperature
I_L : current in coil L
E : input voltage
V_{dc} : output voltage
α : order
L : the inductance of the coil in [H]
C : the capacitance of the capacitor in [F]
R : the resistance of the load R in [Ω].
T_S : is the switching period which is equal 1
F_s : the duty cycle of the switch ($d \in [0, 1]$).
k_r : proportionality coefficient [[Nm] (rd.S⁻¹/)]
C_s : static torque very small [Nm]
ω : rotation speed (rd.S⁻¹)
W : the rotation speed
H_m : the head
H_g : geometric height
Q : volume flow
K_h : given pump constant
R_s : stator phase resistance
R_r : rotor phase resistance
J : Moment of inertia reduced on the machine shaft
T_{em} : electromagnetic torque developed by the machine
C_r : resistant torque of the load
F : viscous friction coefficient
P : the number of poles pairs
P_{elec} : electric power of the asynchronous motor (w)
h : average daily usage time (enh)
U : installation voltage in V
N_p : number of modules in parallel
N : number of modules
P_{cm} : peak power of a module
P_s : it is the surface area of a generator
S : it is the surface area of a module in m²
N : Nombre of module
P_h : hydraulic power [W]
g : acceleration of gravity [9.81m/s²]
H : total head [m]
K : coefficient which varies from 0.75 à 1.4.

$V_{co}N_s$: The sum of the open circuit voltages of N_s cells in series.

$I_{cc}N_s$: Short-circuit current of N_s cells in series.

H_s : static

H_c : kinetic

H_v : frictio

P_1, P_2 : are the pump inlet and outlet pressures.

ρ : is the density of the fluid.

G : is acceleration due to gravity.

V_1, V_2 : are the fluid speeds at the pump inlet and outlet.

F : is the coefficient of pressure loss.

L : is the length of the pipe.

D : is the diameter of the pipe.

P_h : is the hydraulic power supplied by the pump.

P_m : is the mechanical power provided by the engine.

Q : is the volumetric flow of the fluid.

H : is the total manometric height.

ρ : is the density of the fluid.

G : is acceleration due to gravity.

T : is the mechanical torque applied to the pump shaft.

Ω : is the angular velocity of the pump shaft.

L_{as} : Clean inductance of a stator phase.

L_{ar} : Clean inductance of a rotor phase.

Abbreviations

GPV : photovoltaic generator

MPPT: maximum Power Point Tracking.

PPM :point of Maximal power

DTC : the direct torque control

HMT : total manometric height

Abstract



Resumé

Ce projet vise à modéliser et optimiser un système photovoltaïque pour alimenter une station de dessalement rurale. Il intègre des données locales d'ensoleillement et des techniques d'optimisation avancées pour maximiser l'efficacité énergétique et la durabilité du système. Les résultats attendus incluent une réduction des coûts, une amélioration de la fiabilité énergétique et une fourniture durable d'eau potable pour les communautés rurales. Le système proposé est constitué d'un ensemble d'éléments, à savoir le générateur PV, les convertisseurs DC/DC et DC/AC, une pompe immergée entraînée à travers un moteur asynchrone. Afin d'assurer l'extraction de la puissance maximale du générateur photovoltaïque nous avons utilisé l'algorithme de recherche du point de puissance maximale MPPT-P&O et dans le but d'obtenir un contrôle dynamique performant du couple, et de réaliser un découplage entre le couple moteur et le flux nous avons appliqué la commande directe du couple (DTC). Les résultats des simulation ont montré l'autonomie et la robustesse du système étudié.

Abstract

This project aims to model and optimize a photovoltaic system to power a rural desalination plant. It incorporates local sunshine data and advanced optimization techniques to maximize system energy efficiency and durability. Expected results include reduced costs, improved energy reliability and sustainable drinking water supply for rural communities. The proposed system consists of a set of elements, namely the PV generator, the DC/DC and DC/AC converters, a submerged pump driven through an asynchronous motor. In order to ensure the extraction of the maximum power of the photovoltaic generator we used the algorithm of search of the maximum power point MPPT-P&O and in order to obtain an efficient dynamic control of the torque, and to realize a decoupling between the motor torque and the flow we applied the direct control of the torque (DTC). The simulation results showed the autonomy and robustness of the system studied.

ملخص

يهدف هذا المشروع إلى نمذجة وتحسين نظام الطاقة الكهروضوئية لتشغيل محطة تحلية المياه الريفية. يتضمن بيانات أشعة الشمس المحلية وتقنيات التحسين المتقدمة لزيادة كفاءة الطاقة في النظام ومثابته. وتشمل النتائج المتوقعة انخفاض التكاليف وتحسين موثوقية الطاقة واستدامة إمدادات مياه الشرب للمجتمعات الريفية. يتكون النظام المقترح من مجموعة من العناصر، وهي مولد الطاقة الكهروضوئية، ومحولات DC/DC و DC/AC، وهي مضخة مغمورة مدفوعة عبر محرك غير متزامن. من أجل ضمان استخراج الطاقة القصوى للمولد الكهروضوئي، استخدمنا خوارزمية البحث عن نقطة الطاقة القصوى MPPT-P & O ومن أجل الحصول على تحكم ديناميكي فعال في عزم الدوران، ولتحقيق الفصل بين عزم الدوران الحركي والتدفق طبقنا التحكم المباشر في عزم الدوران (DTC) أظهرت نتائج المحاكاة استقلالية ومثابته النظام المدروس.

General introduction



General introduction

Currently, most of the production of electrical energy is based on non-renewable resources such as coal, natural gas, and oil, which represent 81% of the world's energy production in 2009, which will be a few decades from now. In addition, energy demand growth generally results in a fluctuation in the price of oil in the world market. Renewable energies offer the possibility of producing electricity cleanly, especially with less dependence on resources, provided they accept their fluctuations. The main advantage of these renewable energies is that they pollute the atmosphere and do not produce greenhouse gases such as carbon dioxide and nitrogen oxides, which are responsible for global warming.

Solar photovoltaic (PV) energy is increasingly used in various land-based applications such as lighting, telecommunications, refrigeration, and pumping. PV systems do not require any external fuel input; in addition, the generator itself contains no moving parts and therefore hardly requires maintenance. Therefore, recurring operating and maintenance costs are relatively low. For these reasons, this energy source is particularly suitable for rural uses where populations are distributed in small communities with relatively low energy demand.

Today, the use of photovoltaic energy for water pumping is a nascent technology characterized by gradually declining costs. Since the solar water pumping systems provide

Domestic supplies, livestock, and water irrigation in remote areas have enormously gained acceptance, reliability, and performance, and nowadays they belong to the most significant applications of photovoltaic energy. This can be mainly attributed to the fact that it is not economically feasible to link such remote sites to the electric network in this project aims to model and optimize a photovoltaic system to power a rural desalination plant. It integrates local sunshine data and uses advanced optimization techniques to maximize system energy efficiency and durability. Expected results include reduced costs, improved energy reliability and sustainable drinking water supply for rural communities. The proposed system consists of a photovoltaic generator, DC/DC and DC/AC converters, and a submersible pump driven by an asynchronous motor. To ensure the extraction of the maximum power of the photovoltaic generator, we used the MPPT-P&O maximum power point search algorithm. In order to obtain a powerful dynamic torque control and to achieve a decoupling between the engine torque and the flow, we applied the direct torque control. The simulation results showed the autonomy and robustness of the studied system.

it structured in three chapters.

The first chapter is dedicated to highlighting the main devices of photovoltaic systems. Starting with a presentation of renewable energies, including PV photovoltaic generators.

Then, we present the different devices of a PV system used for water pumping, namely the solar cell, the PV module, the PV panel, the DC/DC converters (chopper), and the DC/AC inverter feeding a three-phase IM driving an immigrant centrifugal pump. The modeling of the different components of the photovoltaic pumping system was the subject of the second chapter.

General introduction

The last chapter is the purpose of our work: the dimming of the system. In this part, we will mention the command (DTC) and its operating principle, as well as the simulation of the complete system, and we will present the results of the modeling and simulation of the studied system in order to validate the choice and robustness of the proposed order.

A general conclusion concludes our work.

Chapter I: Photovoltaic Pumping systems

I.1 Introduction

Renewable energy, such as photovoltaic, is the most widespread in the world; it is also environmentally friendly and relies on modern and efficient technologies, which everyone is betting on as a conventional alternative energy source in the near future. This energy is increasingly being used to operate various terrestrial applications such as lighting, refrigeration, and water pumping.

The use of solar pumping systems aims to provide domestic livestock and water irrigation supplies in remote areas. Not only are solar water pumps cost-effective, but they are also environmentally friendly and well suited to the needs of remote communities with good sunshine, such as Algeria, which has one of the highest solar deposits in the world. The objective of this chapter is to give a state-of-the-art overview of photovoltaic pumping systems and an overview of the components that constitute photovoltaic pumping systems.



Fig I.1 Solar livestock pumping systems and water irrigation

Solar energy is converted into electricity by means of photovoltaic cells. The DC/AC converter converts the direct current produced by the solar panels into three-phase alternating current to operate the pump motor group see (Fig I.2). The advantages of the solar pumping system are that it uses clean and sustainable energy, is competitive compared to conventional systems (gasoil and butane), and has a low operating and maintenance cost.

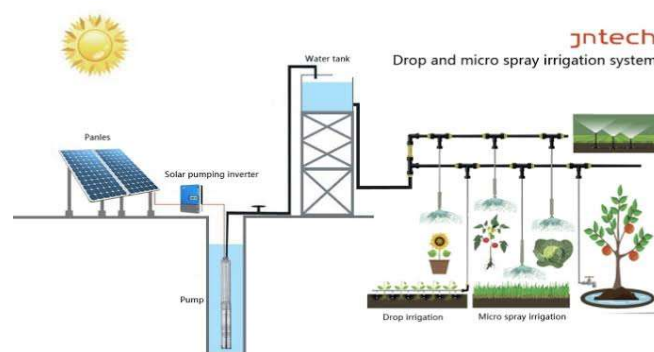


Fig I.2 Conversion steps

I.2 Photovoltaic pumping systems

In rural areas of developing countries, many people face major challenges related to water scarcity, a situation that is particularly critical in desert areas. The issue of water scarcity in these arid regions is of vital importance to the inhabitants, and the improvement of their living conditions is closely linked to the search for appropriate solutions to this pressing problem. Photovoltaic (PV) pumping is the ideal solution to meet water needs in places where traditional electricity networks are lacking. At present, two types of photovoltaic pumping systems are commonly used, those with batteries and those without batteries.

I.2.1 Pumping over the sun

The storage is done hydraulically, where the water is pumped into a tank located above the ground when there is enough sunlight. Subsequently, it is distributed as needed, thanks to gravity. This solar pumping system offers a simpler approach to photovoltaics [1]. However, battery-free technology has some drawbacks, including the dependence of water flow on sunlight throughout the day. Despite this, the operation of this installation remains relatively simple. The tank acts as a temporary buffer while the water is pumped with solar energy. Although this option is less expensive, the pumps do not work effectively under a certain level of brightness, as at the beginning or end of the day, and their efficiency decreases outside their nominal operating range. The solar pump is directly connected to the photovoltaic generator via a DC/DC or DC/AC converter, depending on whether a DC motor or an AC motor is used. This results in a variation in the flow of water into the tank as a function of solar radiation.

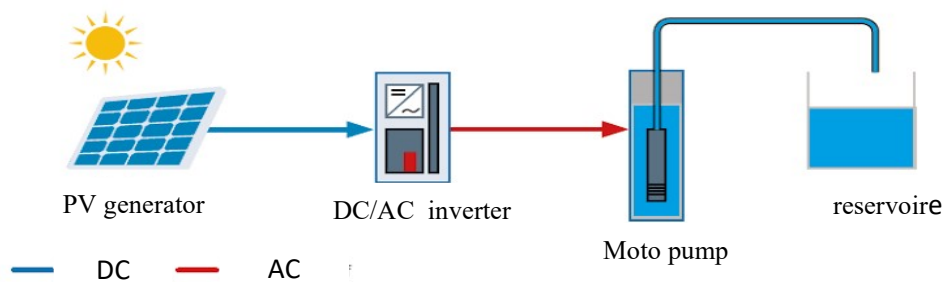


Fig I.3 Working principle of pumping to the sun wire.

I.2.2 Pumping with electrochemical storage (Batteries)

Photovoltaic pumping does not always synchronize perfectly with the hours of sunshine when uniform intensity is required, making storage indispensable. To remedy this, electricity can be stored in batteries and recovered as needed. However, to ensure the longevity of the batteries, a regulator is essential to protect them from deep discharges or overloads. The focus of current research is photovoltaic pumping with batteries, thus offering energy independence and constant flow according to needs [2]. This approach is illustrated in the figure below.



Fig I.4 Photovoltaic pumping with energy storage

I.3 The Photovoltaic System

Solar energy is the energy that the sun emits in the form of heat and light, and it is considered a renewable energy source because it is virtually inexhaustible on the scale of human life. This energy can be used to produce electricity or heat. There are two main methods of solar energy conversion:

- a) Solar thermal energy simply involves the production of heat using dark panels. This heat can be used to generate steam, which in turn can be converted into electricity.
- b) Photovoltaic solar energy is the direct generation of electricity from light using solar panels. This form of energy is already widely used in many countries, especially in those without conventional energy resources such as hydrocarbons or coal [3].

I.3.1 Photovoltaic effect

Solar cells, also called photovoltaic cells, are optoelectronic devices that directly convert light into electricity. They are created using semiconductor components. In most cases, silicon acts as the main ingredient. Amorphous, poly-crystalline or monocrystalline solar cells can be more or less efficient depending on the manufacturing process. Gallium arsenide and cadmium telluride are additional materials that can be used.

I.3.1.1 The photovoltaic cell

The photovoltaic cell is composed of a semiconductor material that absorbs light energy and transforms it directly into electric current [4].

I.3.2 The principal of operation

The conversion of photons absorbed by a semiconductor into carriers of electric charges (electrons and holes) is the basic idea of a photovoltaic cell. Because of the production of charges, an electric current will flow in a circuit connected to the electrodes, and a differences will be created at the terminals of the electrodes, as shown in the figure below:

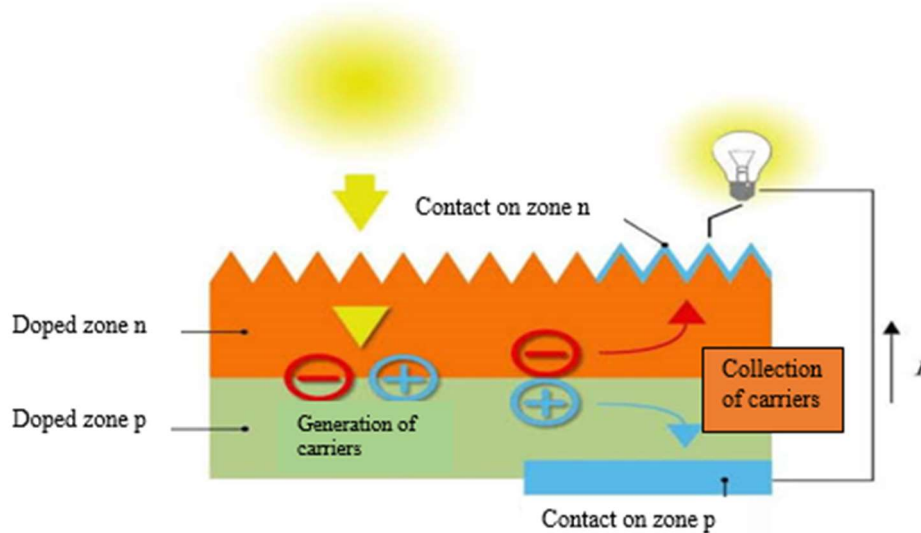


Fig I.5 Principle of operation of a photovoltaic cell

I.3.3 The different types of photovoltaic cells

There are several types of photovoltaic cells. The main ones are:

- Monocrystalline solar cells: Made from a single silicon crystal, they offer high efficiency but are generally more expensive to produce.
- Poly crystalline solar cells: Composed of several silicon crystals, they are less expensive to produce than single crystals, but their yield is slightly lower.
- Amorphous silicon solar cells: Use non-crystalline silicon, which makes them flexible and cheaper to produce. However, they have a lower yield than crystalline cells.
- Thin film solar cells: Manufactured by depositing thin layers of semiconductor materials on a substrate. They are light, flexible and may have a lower cost of production, but their yield may be lower.
- Organic solar cells: Use organic materials to convert light into electricity. They are light, flexible, but generally have a lower yield.

Each type of photovoltaic cell has advantages and disadvantages, and the choice often depends on the specific needs of the project, the budget and the availability of materials .

I.3.4 The photovoltaic module

To increase the operating voltage, photovoltaic (PV) cells are usually connected in series. Thus, the nominal voltage of the module is often adjusted to correspond to a load of 12 volts, which means that the modules usually contain 36 cells. Due to the fragility of the cells against damage and corrosion, they are often protected by a glass or plastic coating. The whole thing, including the cells and their protection, is called a photovoltaic module. In addition, the modules can also be connected in parallel to increase their intensity of use.

a) Serial Association :

A combination of cells in series increases the voltage of the photovoltaic generator (GPV). The cells are then traversed by the same current and the resulting characteristic of the series grouping is obtained by adding the elementary voltages of each cell [5:6].

$$V_{co}N_s = N_s \cdot V_{co} \tag{I.1}$$

$$I_{cc}N_s = I_{cc} \tag{I.2}$$

With :

$V_{co}N_s$: The sum of the open circuit voltages of N_s cells in series.

$I_{cc}N_s$: Short-circuit current of N_s cells in series.

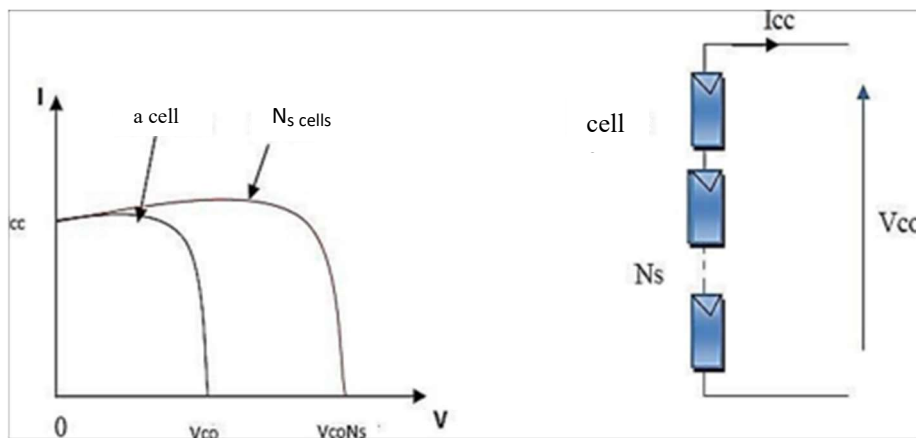


Fig I.6 Characteristic current voltage N_s cell in series

b) Association in parallel

It is possible to associate the cells in parallel, which increases the output current of the generator thus formed. When a group of identical cells is connected in parallel, each cell is subjected to the same voltage and the overall characteristic of the group is obtained by the addition of individual currents.

With :

$I_{cc}N_p$: The sum of the circuit cost currents of (N_p) cell in parallel.

$V_{co}N_p$: The open circuit voltage of (N_p) cell in parallel.

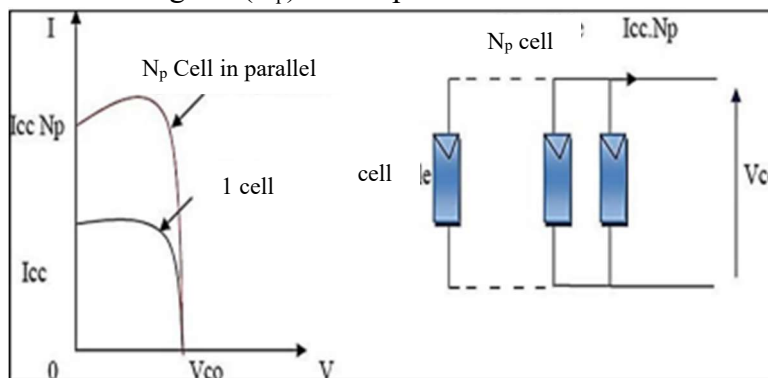


Fig I.7 Characteristic current voltage of (N_p) cells in parallel

I.3.5 Different types of photovoltaic systems

There are generally three types of photovoltaic systems, autonomous systems, hybrid systems and systems connected to a network [7]. The first two are independent of the electricity distribution system, often found in remote areas.

I.3.5.1 Photovoltaic systems connected to the grid

Photovoltaic power generation systems connected to a grid (Fig I.8) are a result of the trend towards decentralization of the grid. Energy is produced closer to where it is consumed. Systems connected to a network reduce the need to increase the capacity of transmission and distribution lines. It produces its own electricity and sends its excess energy to the grid, from which it sources, if necessary. These transfers eliminate the need to buy and maintain a battery. It is still possible to use these systems as backup power when a network failure occurs.

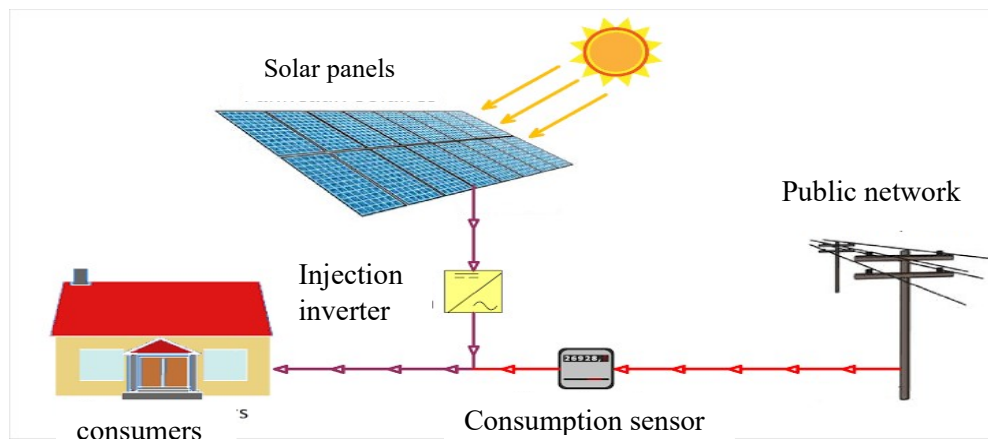


Fig I.8 Photovoltaic system connected to the grid

I.3.5.2 Autonomous photovoltaic systems

These photovoltaic systems are installed to ensure autonomous operation without the use of other energy sources. Generally, these systems are used in remote and isolated areas of the network. Depending on whether electrochemical storage is used, autonomous photovoltaic systems are classified as follows [2]:

I.3.5.2.1 Autonomous systems without electrochemical storage

In this case, the powered device will only work in the presence of sufficient solar illumination for its startup. This is interesting for all applications that do not need to work in the dark and for which the need for energy coincides with the presence of solar illumination. But the photovoltaic generator must be sized so that it has enough power to supply the device with the lowest illumination. Photovoltaic pumping is an example of this category of autonomous systems.

I.3.5.2.2 Stand-alone systems with electrochemical storage

This is the most common configuration of autonomous photovoltaic systems; it includes batteries that store the electrical energy produced by the photovoltaic generator during the day. Therefore, electrochemical storage in batteries is essential to ensure nighttime operation or a predefined number of days in the sizing of photovoltaic systems.

I.4 Solar energy in Algeria

Algeria has one of the highest solar deposits in the world. The duration of insolation over almost the entire national territory exceeds 2000 hours annually and can reach 3900 hours (highlands and sahara). The energy received daily on a horizontal surface of 1 m² is of the order of 5 KWh on most of the national territory, that is, nearly 1700 KWh/m²/year in the north and 2263 KWh/m²/year in the south of the country [3].

Tabel I.1 Solar energy potential in Algeria

	Coastal regions	Highlands	Sahara
Area	4	10	86
Average duration of sunshine (h/year)	2650	3000	3500
Average energy received (KWh/m ² /year)	1700	1900	2650

With a solar field that exceeds 5 billion GWh, our country has also implemented initiatives to promote solar electricity, especially in the context of decentralized electrification. The map below shows the solar radiation

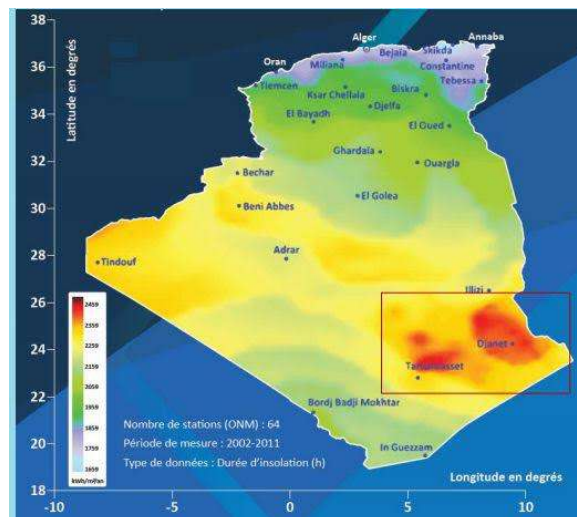


Fig I.9 Preliminary map of solar irradiations in Algeria

I.5 Photovoltaic generator

The photovoltaic generator is formed by a set of modules, which consist of different solar cells connected in series and in parallel to produce the necessary current and voltage. The performance of the generator is determined by the diversity of the component units and the cells that constitute them. The number of units connected in series sets the output voltage of the solar generator, while the number of units connected in parallel determines the output current. The term "PV field" refers to the combined group of photovoltaic modules.

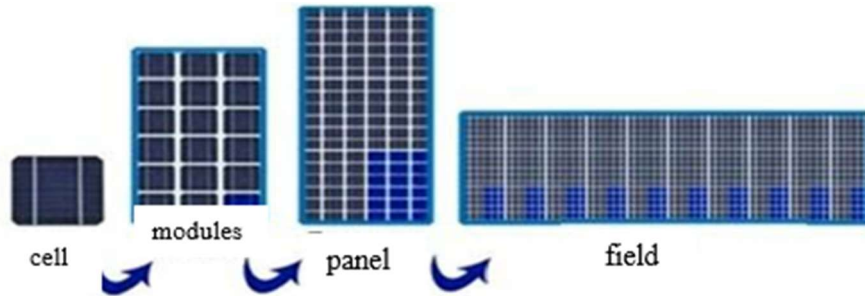


Fig I.10 Components of a photovoltaic module generator

I.6 Static converters used in photovoltaic pumping systems

Static converters are systems that adapt the electrical energy source to a given receiver. Depending on the type of machine to be controlled and the nature of the power source, there are several families of static converters.

I.6.1 DC/DC Converter (Chopper)

DC/DC converters whose function is to provide variable DC voltage from a fixed DC voltage. This energy conversion is achieved through a high frequency "switching" characterized by high efficiency [8].

I.6.1.1 Buck Converter (Series Chopper)

The Buck converter, also known as the series chopper, turns one DC voltage into another lower DC voltage. The L and C components form a filter to mitigate fluctuations resulting from switching on the output voltage and current.

The switch S is activated for a fraction αt of the switching period T. The power source supplies power to the inductor L. When S is deactivated, the freewheel diode D ensures continuity of current and allows L to discharge.

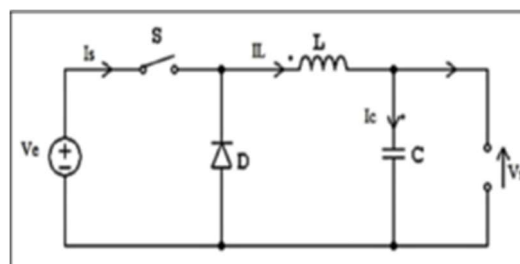


Fig I.11 The schematic of the series chopper

I.6.1.2 Boost Converter (Parallel Chopper)

A Boost converter, or parallel chopper, converts a DC voltage into another DC voltage of higher value. The inductance allows to smooth the current called on the source. The capacity C allows to limit the ripple of voltage in output.

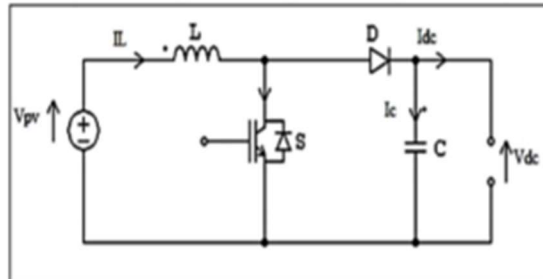


Fig I.12 The schematic of the parallel chopper

I.6.1.3 DC/AC Converter (Inverter)

Static circuits called inverters converting the AC power to the desired voltage, current and frequency. The output voltage of an inverter has a non-synoidal periodic waveform that can be quite close to the required waveform. The three-phase inverter is made by the combination, in parallel, of three single-phase inverters in half bridge (or bridge) giving three output voltages out of phase of 120 degrees, one compared to wish [9].

I.7 Motor-pump unit

A motor pump is a set consisting of an electric motor driving a hydraulic pump.

I.7.1 Motors (IM)

The motor of a pump unit converts electrical energy into mechanical energy. It can be direct or alternating current. In this work, the asynchronous machine is used because it is the most reliable of the electrical machines, the most robust of its generation, and the least expensive to manufacture. In this case, an electronic converter or inverter is needed to convert the direct current from a photovoltaic generator to alternating current [2]. The IM is an AC machine for which the rotation speed of the shaft is different from the rotation speed of the rotating field. The machine that interests us in this part is, more precisely, an induction machine.

I.7.2 The Pumps

A pump is a hydraulic machine that draws and discharges a liquid (water, oil, gasoline, food liquids, etc.) from a point to a desired location. The pump is intended to raise the charge of the pumped liquid. The charge or energy is the sum of three energy categories:

- Kinetic energy $V^2/2g$
- Potential energy H or Z .
- Pressure energy $P/\rho g$.

The pump is a device that generates a pressure difference Δp between the input and output of the machine, the energy required to operate a pump depends on:

- Fluid properties : density ρ , dynamic viscosity μ .
- Flow characteristics : pressure, velocity V , flow rate Q , height H .
- Facility characteristics : pipe length L , diameter D , and absolute roughness [10].

I.7.2.1 Types of pumps

Water pumps are usually classified according to their working principle, either volumetric or centrifugal. In addition to these two classifications, two other types of pumps are distinguished according to the physical location of the pump in relation to the pumped water : the suction pump and the discharge pump [11].

a) Positive displacement pumps : The positive displacement pump transmits the kinetic energy of the moving motor allowing the fluid to overcome gravity by successive variations of a volume connected alternately to the suction port and the discharge port.

b) Centrifugal pumps : centrifugal pumps are the most common in the field of water pumping. They are coupled with the a IM constituting an electric pump.

I.7.3 The centrifugal pump

The centrifugal pump is designed for a relatively fixed total manometric height (HMT). The flow rate of this pump varies in proportion to the speed of rotation of the motor. Its torque increases very quickly according to this speed and the discharge height is a function of the square of the motor speed. The speed of rotation of the engine will therefore have to be very fast to ensure a good flow. The power consumption, proportional to $Q \cdot HMT$, will therefore vary in the ratio of the speed cube. Centrifugal pumps will usually be used for high flow rates and medium or low depths (10 to 100 metres).

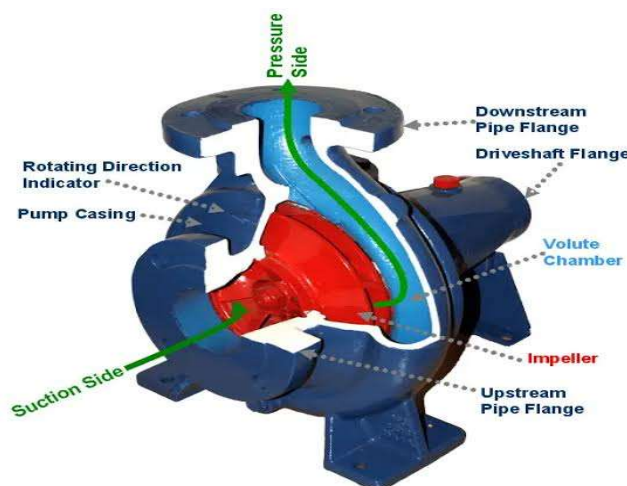


Fig I.13 View in front of a centrifugal pump

The pump consists of two essential components :

-A wheel that forces the liquid to rotate. The wheel is mounted on a shaft supported by bearings and driven by an engine.

- A pump body that directs the flow to the impeller and moves it away again under higher pressure. The pump body includes suction and discharge tubing, supports the bearings and the rotor assembly.

The centrifugal pump transmits the kinetic energy of the motor to the fluid through a rotation movement of impellers or fins. The water enters the center of the pump and is pushed outwards and upwards thanks to the centrifugal force of the vanes. The movement of the liquid results from the increase of energy which is communicated to it by the centrifugal force.

The centrifugal pump is designed for a relatively fixed manometric height (HMT). The flow rate of this pump varies in proportion to the speed of rotation of the motor. Its torque increases very quickly according to this speed and the discharge height is a function of the square of the motor speed. Centrifugal pumps are usually used for high flow rates and medium to low depths (10 to 100 metres). Below is an illustration of a centrifugal pump.

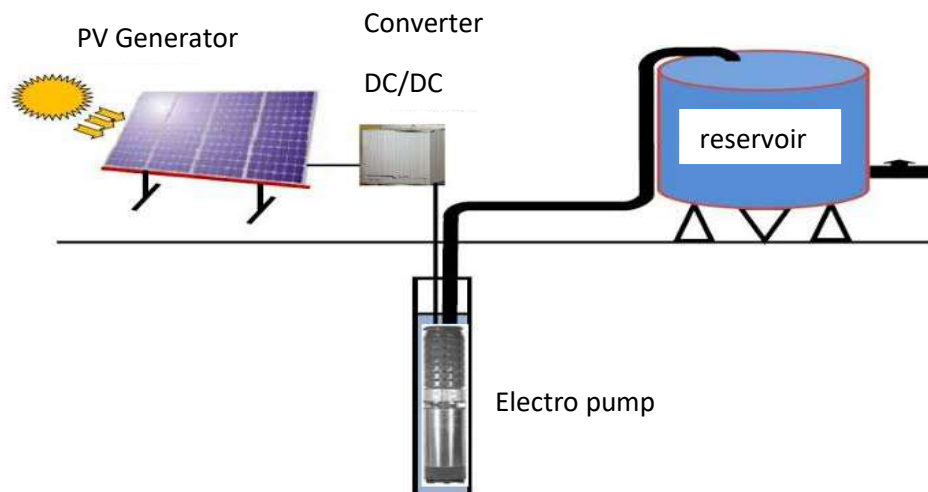


Fig I.14 Example of installation with a centrifugal pump

I.8 Conclusion

We have presented in this chapter general information on the photovoltaic pumping system and solar energy (sunshine, photovoltaic effect, etc.), as well as the elements constituting the photovoltaic pumping system. The photovoltaic pumping system that we will study in the following chapters II and III consists of a photovoltaic generator, converters (choppers, voltage inverters), and the asynchronous motor of a centrifugal pump.

Chapter II: Modelling of Photovoltaic Pumping System

II.1 Introduction

The modeling of a physical system leads to the establishment of mathematical equations governing the dynamics of this system; hence, a model is the mathematical representation of a real entity's functioning. When one has a model, we can simulate the behavior of this entity. In this chapter, we will model a photovoltaic pumping system that consists of three floors. The first is a photovoltaic generator connected to an elevator converter (DC/DC) that ensures maximum power operation. The second represents a voltage source inverter that converts direct current to alternating current with indirect vector control. The third part is the induction motor, which drives the pump to extract water.

II.2 Photovoltaic solar energy

Photovoltaic solar energy is a renewable source of electricity from solar radiation, resulting from nuclear fusion in the heart of the Sun. This electromagnetic radiation propagates through the solar system in the form of photons. Photovoltaic cells exploit the photoelectric effect, grouped into solar modules that, in turn, form installations capable of producing electricity that can be used locally or to power a grid. The Earth receives a constant solar power of 170 million gigawatts, of which 122 are absorbed. For maximum use, photovoltaic modules should ideally be oriented perpendicular to the sun's rays, but this optimal orientation depends on the variability of the solar position over time

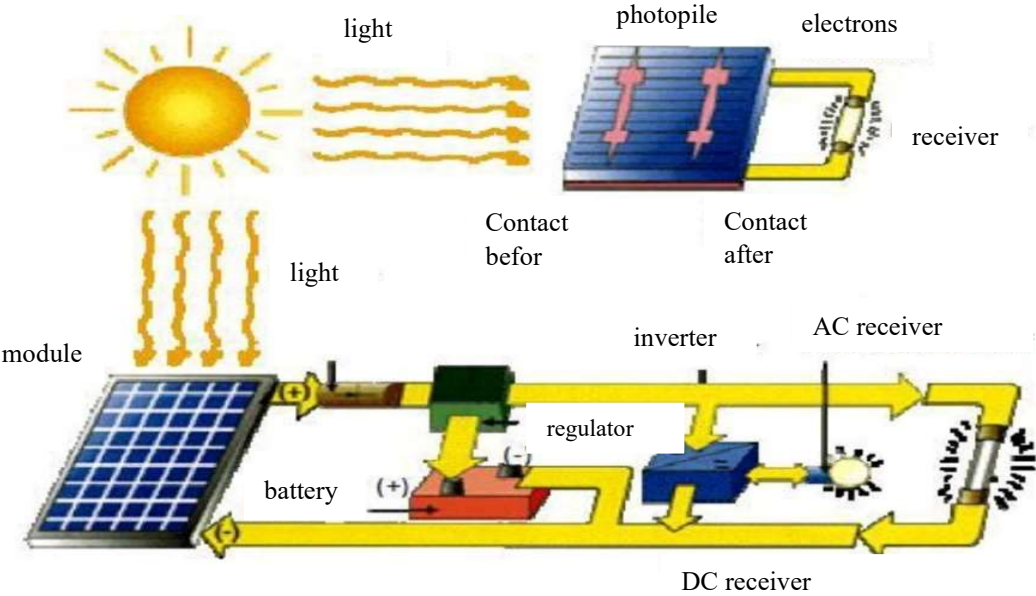


Fig II.1 photovoltaic system

II.2. 1 Modelling of the power system

The power system is represented by a photovoltaic generator connected to an elevator converter (DC/DC) which ensures maximum power operation by adjusting the cyclic ratio via MPPT control techniques to reach its maximum value with available radiation.

II.2.2 Modelling of the photovoltaic generator

The diagram of the equivalent circuit of a photovoltaic cell, which is widely used in the literature, is shown in (Fig II.2). This model is used to study the current-voltage (I-V) and power-voltage (P-V) characteristics of the photovoltaic generator as well as its behavior according to solar parameters, namely the illumination in the plane of the panels and the junction temperature [12].

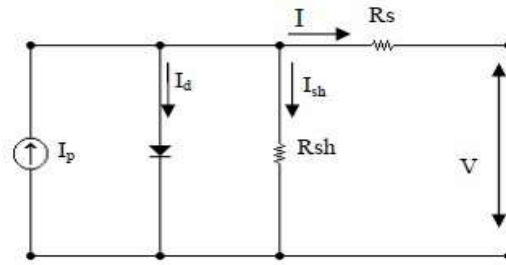


Fig II.2 Modelling of the equivalent electrical circuit of a PV cell [20]

In (Fig II.2), the resistance characterizes the leakage current at the junction and the resistance represents the various contact and connection resistors [13]. The current generated by the module is given by Kirchoff's law as follows:

$$I = I_p - I_d - I_{sh} \quad (II.1)$$

with:

I : The current delivered by the module.

I_d : Diode current.

I_{sh} : The shunt current.

The current I_p depends directly on the solar radiation E_s and the temperature of the cell T_j , it is given by the following relation [15].

$$I_p = P_1 \cdot E_s \left[1 + P_2 (E_s - E_{ref}) + (P_3 (T_j - T_{jref})) \right] \quad (II.2)$$

The cell temperature can be calculated from the ambient temperature and the irradiation temperature as follows:

$$T_j = T_a + E_s \left(\frac{N_{oct} - 20}{800} \right) \quad (II.3)$$

or:

T_a : Room temperature.

N_{oct} : The manufacturer's rated cell operating temperature condition (45°C). The diode current is given by:

$$I_d = I_{sat} \left[\exp \left(\frac{q(V.R_s.I)}{N_s.A.K.T_j} \right) - 1 \right] \quad (II.4)$$

with:

I_{sat} : Saturation current, it is strongly temperature dependent; it is given by the following expression:

$$I_{sat} = P_4 \cdot T_j^3 \cdot \exp \left(\frac{-E_g}{k.T_j} \right) \quad (II.5)$$

The shunt resistor current is calculated by:

$$I_{sh} = \frac{V.R_s.I}{R_{sh}} \quad (II.6)$$

Module I current is given by:

$$I = I_p(E_s, T_j) - I_d(V, I, T_j) - I_{sh}(V) \quad (II-7)$$

$$I = P_1 \cdot E_s \cdot \left[1 + P_2 \cdot (E_s - E_{ref}) + P_3 \cdot (T_j - T_{ref}) \right] - P_4 \cdot T_j^3 \cdot \exp \left(\frac{-E_g}{k.T_j} \right) \cdot \left[\exp \left(\frac{q(V.R_s.I)}{N_s.A.K.T_j} \right) - 1 \right] - \frac{(V_{pv} + R_{SI})}{R_{sh}} \quad (II-8)$$

The block diagram of the photovoltaic generator is shown in Figure (II.3), with:

- The two input variables are solar in the panel plane (W/m^2) and cell junction temperature ($^{\circ}C$).
- The two output variables are: I current supplied by the GPV (A) and V voltage at the GPV terminals (V).

II.2.3 Electrical modelling of a photovoltaic cell

The equivalent scheme of a photovoltaic cell under illumination is shown in (Fig II.3) It represents an I_{ph} current generator in parallel with a diode, and incorporates two parasitic resistors. These resistances influence the characteristic $I = f(V)$ of the cell [14]:

The series resistance (R_s) represents the internal resistance of the cell, depending mainly on the semiconductor used, the contact resistance of the collector grids, and the resistivity of

these grids. The shunt resistance (R_{sh}) is related to a leakage current at the junction, and its influence depends on how this junction was realized.

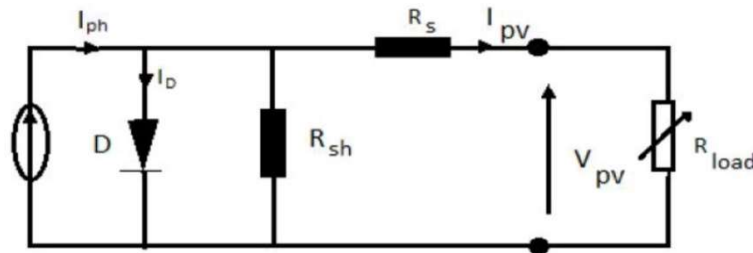


Fig II.3 Equivalent scheme of a photovoltaic cell under illumination

The mathematical model for the current-voltage characteristic of a PV cell is given by:

$$I_{pv} = I_{ph} - I_{sat} * \left[e^{\left(q * \frac{V_{pv} + R_s * I_{pv}}{n * K * T_c} \right)} - 1 \right] - \frac{V_{pv} + R_s * I_{pv}}{R_{sh}} \quad (II.9)$$

Where I_{sat} is the saturation current, K is the Boltzmann constant ($1,3811023 \text{ J/K}$), T is the effective temperature of the cells in Kelvin(K), e is the charge of the electron ($e=1,6 \cdot 10^{-19} \text{ C}$), n is the ideality factor of the junction ($1 < n < 3$), I_{pv} is the current supplied by the cell when it operates in generator, V_{pv} is the voltage at the terminals of this same cell, I_{ph} is the photo-current of the cell depending on the illuminance and temperature or current of (short circuit), R_{sh} is the shunt resistance characterizing the leakage currents of the junction, R_s is the serial resistance representing the various resistances of contacts and connections

II.2.3 Parameters of a photovoltaic cell

These parameters can be determined from current-voltage curves, or from the characteristic equation. The most common are:

II.2.3.1 Short Circuit Current (I_{cc})

This is the current for which the voltage at the terminals of the cell or PV generator is zero. In the ideal case (R_s null and R_{sh} infinite), this current merges with the photo current I_{ph} otherwise, by cancelling the voltage V in equation (1), we obtain:

$$I_{sat} * \left[e^{\left(q * \frac{R_s * I_{cc}}{n * k * T_c} \right)} - 1 \right] - \frac{R_s * I_{cc}}{R_{sh}} \quad (II.10)$$

Cells (don't the resistance series is low), one can neglect the term before I_{ph} . The approximate expression of the short-circuit current is then: quantitatively, it has the largest value of the current generated by the cell (practically) .

$$I_{cc} = \frac{I_{ph}}{1 + \frac{R_s}{R_{sh}}} \quad (\text{II.11})$$

With $I_{cc} = I_{ph}$.

II.2.3.2 Open circuit voltage (V_{co})

This is the V_{co} voltage for which the current output by the photovoltaic generator is zero (this is the maximum voltage of a photopile or a photovoltaic generator).

$$0 = I_{ph} - I_{sat} * \left[e^{\left(q * \frac{V_{pv}}{nKT_c} \right)} - 1 \right] - \frac{V_{pv}}{R_{sh}} \quad (\text{II.12})$$

In the ideal case, its value is slightly lower than

$$V_{co} = V_{th} * I_n \left[\frac{I_{ph}}{I_{sat}} + 1 \right] \quad (\text{II.13})$$

II.2.4 Advantages and disadvantages of PV system

a) The benefits

- High reliability is the first feature. The absence of moving parts in the facility makes it particularly suitable for remote areas, hence its frequent use in spacecraft.
- The modularity of the photovoltaic panels allows a simple and adaptable assembly to various energy needs. These systems can be sized for applications ranging from milliwatt to megawatt.
- The operating cost is very low due to reduced maintenance, and it does not require fuel, transportation, or highly specialized personnel.
- From an ecological point of view, photovoltaic technology has advantages, as the final product is non-polluting, silent and does not cause any environmental disturbance, except that related to the occupation of space for large installations

b) The disadvantages

The actual conversion rate of a photovoltaic module is low, usually around 10 to 15% (corresponding to about 10 to 15 MW/km² for the BENELUX), with a theoretical limit of 28% for a cell. Photovoltaic generators compete with diesel generators only for low energy demands in remote areas, and their performance is dependent on weather conditions. When energy storage in chemical form (a battery) is required, this leads to an increase in generator costs. In addition, the storage of electrical energy still presents many challenges. The low efficiency of photovoltaic panels is explained by the functioning of the cells, which require a minimum energy of 1 eV to move an electron. Incident rays with energy below 1 eV are not converted into electricity, while those with energy above 1 eV lose some of this energy, with the rest dissipating as heat.

II.3 The statistical converters

In a renewable energy conversion system, converters are used to charge storage batteries and to convert direct current to alternating current, and vice versa. Renewable energies often involve three types of converters: rectifiers, inverters and choppers. The study of these converters is important, because they are widely used in new grid-connected power generation sources, such as wind, photovoltaic and fuel cells , we present the different types of static converters that can be used in the photovoltaic system. We start with the converters (DC-DC) and their different types, then approach the converters (DC-AC). This chapter also exposes some MPPT methods based on the power reaction, such as the inductance incrementing algorithm and the perturbation and observation method

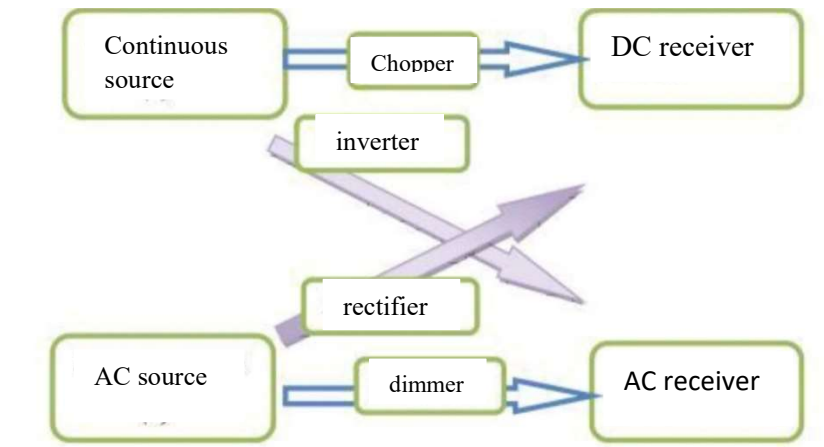


Fig II.4 the different types of static converters

II.3.1 Boost chopper

A boost chopper, also called a lift converter, is an electronic device that converts a low level DC voltage to a higher level DC voltage. It uses a switching configuration to increase the input voltage, thus achieving a higher output voltage than the input voltage. This type of chopper is commonly used in applications requiring increased voltage, such as power supplies and battery charging systems

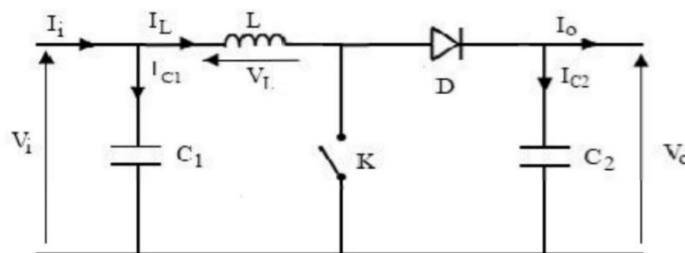


Fig II.5 Electrical diagram of a boost chopper

II.3. 2 Operation of a boost choper

When the switch is closed, the current in the inductance increases linearly. The voltage at the K terminals is zero during this period. When the switch opens, the energy stored in the inductance guides the current through the freewheel diode D. By expressing that the voltage at the terminals of the inductance is zero, one obtains $V_0 (1 - D) = V_i$.

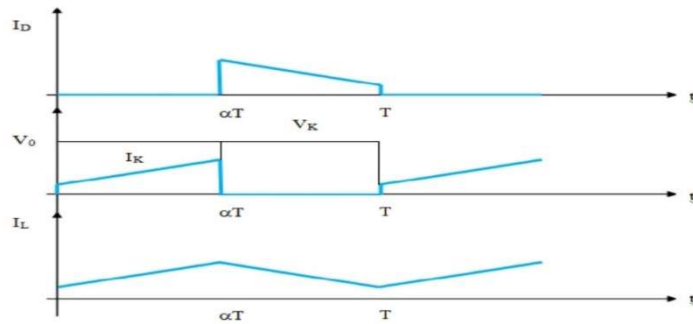


Fig II.6 Chronograms of current and voltage of a boost chopper

II.3.3 Equivalent mathematical models

In order to be able to synthesize the functions of the chopper boost in equilibrium, it is necessary to present the equivalent diagrams of the circuit at each position of the switch K. that of the (Fig II.7) presents the equivalent circuit of the boost when K is Closed c-i.e. between $[0.DT_e]$

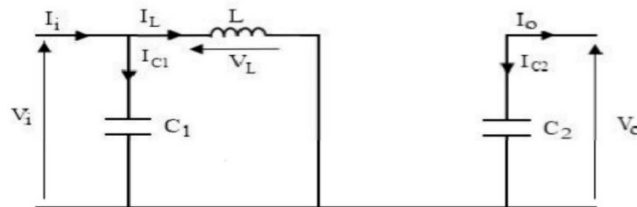


Fig II.7 Electrical diagram of a closed boost chopper

As for the buck circuit, the application of Kirchhoff's laws on the circuits equivalent of the two operating phases give the following calculations

$$I_{c1}(t) = c_1 \frac{dvi(t)}{dt} = I_i(t) - I_l(t) \tag{II.14}$$

$$I_{c2}(t) = c_2 \frac{dv0(t)}{dt} = -I_0(t) \tag{II.15}$$

$$v(t) = L \frac{diL(t)}{dt} = Vi(t) \tag{II.16}$$

The open state of the switch K, the circuit equivalent to the operation of the Boost is the next:

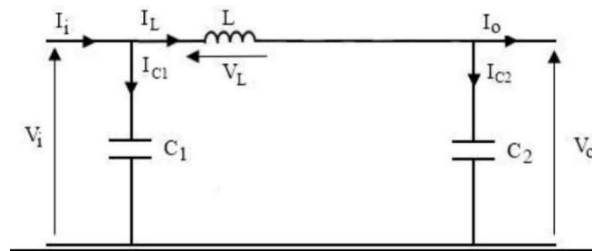


Fig II.8 Electrical diagram of an open boost chopper

$$I_{C1}(t) = c_1 \frac{dV_L(t)}{dt} = I_i(t) - I_L(t) \tag{II.17}$$

$$I_{C2}(t) = c_2 \frac{dV_o(t)}{dt} = I_L(t) - I_o(t) \tag{II.18}$$

$$V_L(t) = L \frac{dI_L(t)}{dt} = V_i(t) - V_o(t) \tag{II.19}$$

II.4 Principle of operation of an inverter

An inverter is an electronic device that performs the static conversion of a voltage/direct current to a voltage/alternating current. It is considered autonomous if it can generate its own frequency and waveform. To achieve this conversion.

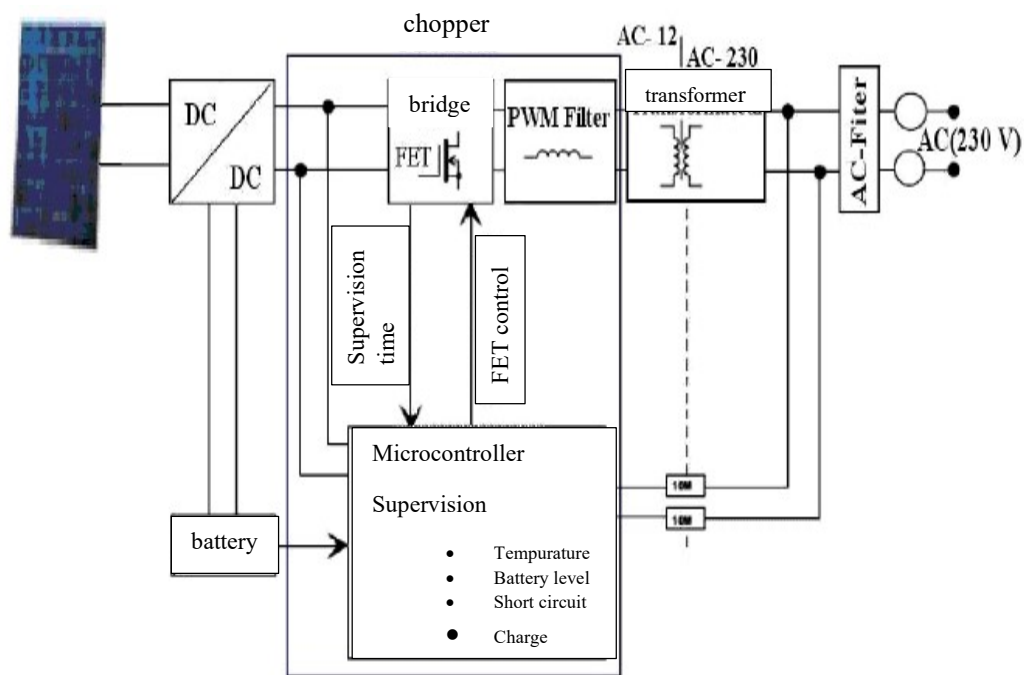


Fig II.9 Inverter operation diagram

II.4.1 Three-phase inverter

This type of inverter is generally recommended for large applications power. The structure of such converter is made by the association, in parallel, of three Single-phase inverters in half bridge (or bridge) giving three output voltages out of phase 120 degrees from each other

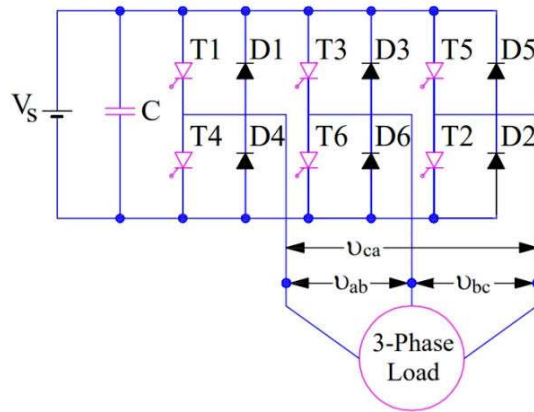


Fig II.20 Schematic diagram of a three-phase bridge inverter

This figure shows the topology of a three-phase inverter with six power switches. The offset between control signals is 60° .

II.5 Inverter Modelling

II.5.1 Voltage Inverter Model

To simplify the study, it is assumed that:

- Switch switching is instantaneous.
- Voltage drop at switch terminals is negligible.
- The three-phase load is balanced, star coupled with an isolated neutral .
- Switches are fully controllable.
- To avoid an arm short circuit and to avoid opening a phase of an inductive load ($F1=1-F1$).

On the basis of these hypotheses, the simplified diagram in (Fig II.22) is obtained.

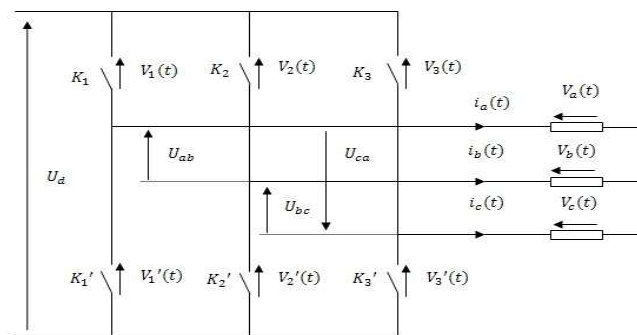


Fig II.22 Simple model of the three-phase inverter

$V_a(t), V_b(t), V_c(t)$: The simple volts delivered by the inverter.

$U_{ab}(t), U_{bc}(t), U_{ca}(t)$: The compound voltages delivered by the inverter.

Compound voltage equations are given by the following relationships:

$$\begin{cases} U_{ab} = V_a - V_b \\ U_{bc} = V_b - V_c \\ U_{ca} = V_c - V_a \end{cases} \quad (\text{II.15})$$

On the other hand, we have the relations between simple tensions and compound tensions as follows:

$$\begin{cases} V_a = \frac{1}{3}(U_{ab} - U_{ac}) \\ V_b = \frac{1}{3}(U_{bc} - U_{ab}) \\ V_c = \frac{1}{3}(U_{ca} - U_{bc}) \end{cases} \quad (\text{II.16})$$

The hypothesis of a balanced voltage system implies:

$$V_a + V_b + V_c = 0 \quad (\text{II.17})$$

The switches K_j , K_j , (1, 2, 3) are unidirectional in voltage and bidirectional in current.

Each UPS arm is assigned a logical F_j ($j = 1, 2, 3$) connection function corresponding to the switch control signals. F_j ($j = 1, 2, 3$) is defined as:

$$f_1 = \begin{cases} 1 & \text{si } K_j \text{ close} \\ 0 & \text{si } K_j \text{ open} \end{cases} \quad (j = 1, 2, 3) \quad (\text{II.18})$$

$$\begin{cases} \text{si } f_1 = 1 \rightarrow V_1 = 0 \\ \text{si } f_1 = 0 \rightarrow V_1 = U_f \end{cases} \rightarrow V_1 = -(f_1 - 1) \cdot U_f \quad (\text{II.19})$$

$$\begin{cases} \text{si } f_2 = 1 \rightarrow V_2 = 0 \\ \text{si } f_2 = 0 \rightarrow V_2 = U_f \end{cases} \rightarrow V_2 = -(f_2 - 1) \cdot U_f \quad (\text{II.20})$$

$$\begin{cases} \text{si } f_3 = 1 \rightarrow V_3 = 0 \\ \text{si } f_3 = 0 \rightarrow V_3 = U_f \end{cases} \rightarrow V_3 = -(f_3 - 1) \cdot U_f \quad (\text{II.21})$$

Let us express the compound voltages according to the logical states of the switches:

$$U_{ab} = V_2 - V_1 \rightarrow U_{ab} = (f_1 - f_2) \cdot U_f$$

$$U_{bc} = V_2 - V_3 \rightarrow U_{bc} = (f_2 - f_3) \cdot U_f \quad (\text{II.22})$$

$$U_{ca} = V_1 - V_3 \rightarrow U_{ca} = (f_3 - f_1) \cdot U_f$$

This gives the following matrix form:

$$\begin{bmatrix} U_{ab} \\ U_{bc} \\ U_{ca} \end{bmatrix} = U_f \cdot \begin{bmatrix} 1 & -1 & 0 \\ 0 & 1 & -1 \\ -1 & 0 & 1 \end{bmatrix} \cdot \begin{bmatrix} f_1 \\ f_2 \\ f_3 \end{bmatrix} \quad (\text{II.23})$$

This gives the following matrix form:

$$\begin{bmatrix} V_a \\ V_b \\ V_c \end{bmatrix} = \frac{1}{3} \cdot \begin{bmatrix} 1 & 0 & -1 \\ -1 & 1 & 0 \\ 0 & -1 & 1 \end{bmatrix} \cdot \begin{bmatrix} U_{ab} \\ U_{bc} \\ U_{ca} \end{bmatrix} \quad (\text{II.24})$$

Replacing (II.22) in (II.23) will have the matrix system (II.24) as follows:

$$\begin{bmatrix} V_a \\ V_b \\ V_c \end{bmatrix} = \frac{1}{3} U_f \cdot \begin{bmatrix} 2 & -1 & -1 \\ -1 & 2 & -1 \\ -1 & -1 & 2 \end{bmatrix} \cdot \begin{bmatrix} f_1 \\ f_2 \\ f_3 \end{bmatrix} \quad (\text{II.25})$$

II.6 IM Modelling

The modeling of the IM is crucial for its development. This chapter presents and models, specifically, the motor operation of an asynchronous cage motor. The housing surrounds the stator circuit with notches, housing a polyphase stator winding. Inside the hollow cylinder of the magnetic circuit, separated by an air gap, is the rotor magnetic circuit housing the cast aluminum or copper bars of the rotor cage. These bars are short-circuited at the ends by rings of the same material. The shaft passes through the rotational magnetic circuit, resting on bearings mounted in the flanges attached to the housing..

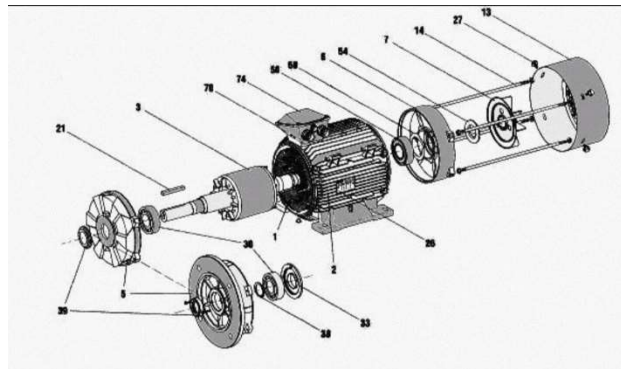


Fig II.23 asynchronous motor

II.6.1 Dynamic modelling

II.6.1.1 Advantages of the IM

The cage asynchronous motor is widely used in industry because of its robustness, reliability and economy. Its high standardisation is also a welcome asset.

II.6.1.2 IM problem

In the IM, stator current is essential for the simultaneous generation of flow and torque. The natural coupling of the DC machine is absent, and access to the internal variables of the cage rotor (such as I_r) is only through the stator. The inaccessibility of the rotor obliges us to adjust the rotoric vector equation in order to express the amplitude through the action on the stator. Structural simplicity masks functional complexity resulting from engine characteristics, nonlinearities, identification challenges and parameter variations, especially R_r up to 100%.

II.6.2 Simplifying Assumptions

The mathematical model of the induction machine is based on several hypotheses, including a perfect symmetry of construction, the assimilation of the cage to a short-circuit winding with the same number of phases as the stator winding, a sinusoidal distribution along the air gap of the magnetic fields of each winding, and the absence of saturation in the magnetic circuit. These conditions make it possible to establish to establish matrix equations for electrical circuits, integrating own and mutual inductances to define flows according to currents.

$$\begin{bmatrix} V_{s\alpha} \\ V_{sb} \\ V_{sc} \end{bmatrix} = \begin{bmatrix} R_s & 0 & 0 \\ 0 & R_s & 0 \\ 0 & 0 & R_s \end{bmatrix} \begin{bmatrix} i_{s\alpha} \\ i_{sb} \\ i_{sc} \end{bmatrix} + \frac{d}{dt} \begin{bmatrix} \varphi_{s\alpha} \\ \varphi_{sb} \\ \varphi_{sc} \end{bmatrix} \quad (II.26)$$

For the rotor:

$$\begin{bmatrix} V_{r\alpha} \\ V_{rb} \\ V_{rc} \end{bmatrix} = \begin{bmatrix} R_s & 0 & 0 \\ 0 & R_s & 0 \\ 0 & 0 & R_s \end{bmatrix} \begin{bmatrix} i_{s\alpha} \\ i_{sb} \\ i_{sc} \end{bmatrix} + \frac{d}{dt} \begin{bmatrix} \varphi_{s\alpha} \\ \varphi_{sb} \\ \varphi_{sc} \end{bmatrix} = \begin{bmatrix} 0 \\ 0 \\ 0 \end{bmatrix} \quad (II.27)$$

The equations of flows as a function of currents are obtained from the matrix [L (θ)], this has 36 non-nuls coefficients, so half depends on time

$$\begin{bmatrix} \varphi_{s\alpha} \\ \varphi_{sb} \\ \varphi_{sc} \\ \varphi_{r\alpha} \\ \varphi_{rb} \\ \varphi_{rc} \end{bmatrix} = \begin{bmatrix} 1 & M_s & M_s & M_1 & M_3 & M_2 \\ M_s & I_s & M_s & M_2 & M_1 & M_3 \\ M_s & M_s & I_s & M_3 & M_2 & M_1 \\ M_1 & M_2 & M_3 & I_r & M_r & M_r \\ M_3 & M_1 & M_2 & M_r & I_r & M_r \\ M_2 & M_3 & M_1 & M_r & M_r & I_r \end{bmatrix} \begin{bmatrix} i_{s\alpha} \\ i_{sb} \\ i_{sc} \\ i_{r\alpha} \\ i_{rb} \\ i_{rc} \end{bmatrix} \quad (II.28)$$

via the electric angle θ, which represents the position of the rotor phase (ra) with respect to the stator phase(sa)

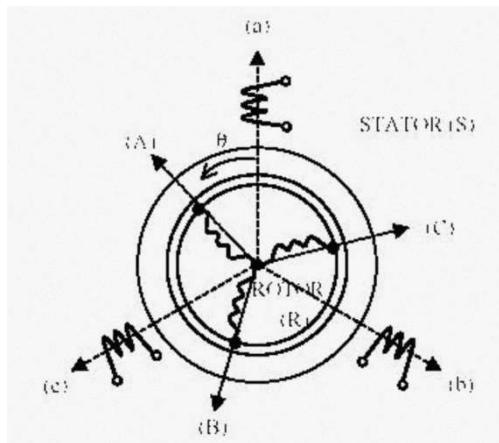


Fig II.24 stator schema

The matrix [L(θ)] shows four submatrices of inductance:

$$\begin{bmatrix} \varphi_{sabc} \\ \varphi_{rabc} \end{bmatrix} = \begin{bmatrix} [L_s] & [M_{sr}] \\ [M_{rs}] & [L_r] \end{bmatrix} \begin{bmatrix} i_{sabc} \\ i_{rabc} \end{bmatrix} \quad (II.29)$$

With

$$[L(\theta)] = \begin{bmatrix} [L_s] & [M_{sr}] \\ [M_{rs}] & [L_r] \end{bmatrix} \quad (II.30)$$

Where the matrix of stator inductors]LS The matrix of L_R rotor inductors

$$[L_r] = \begin{bmatrix} I_r & M_r & M_r \\ M_r & I_r & M_r \\ M_r & M_r & I_r \end{bmatrix} \quad (\text{II.31})$$

$$[L_s] = \begin{bmatrix} I_s & M_s & M_s \\ M_s & I_s & M_s \\ M_s & M_s & I_s \end{bmatrix} \quad (\text{II.32})$$

The matrix of mutual inductances is written

$$[M_{sr}] = [M_{rs}]^r = M_0 \begin{bmatrix} \cos \theta & \cos\left(\theta + \frac{2\pi}{3}\right) & \cos\left(\theta - \frac{2\pi}{3}\right) \\ \cos\left(\theta - \frac{2\pi}{3}\right) & \cos \theta & \cos\left(\theta + \frac{2\pi}{3}\right) \\ \cos\left(\theta + \frac{2\pi}{3}\right) & \cos\left(\theta - \frac{2\pi}{3}\right) & \cos \theta \end{bmatrix} \quad (\text{II.33})$$

Star couplings between coils allow the following relationships to be introduced:

$$i_{s\alpha} + i_{sb} + i_{sc} = 0 \quad \text{and} \quad i_{r\alpha} + i_{rb} + i_{rc} = 0 \quad (\text{II.34})$$

Using 1.9 Grouping terms allows writing A1

$$L_s = I_s - M_s \quad L_r = I_r - M_r \quad \text{and} \quad L_m = \frac{3}{2} M_0 \quad (\text{II.35})$$

The result is:

$$\begin{aligned} [v_{sabc}] &= [R_s][i_{sabc}] + \frac{d}{dt} \{ [L_s][i_{sabc}] + [M_{sr}][i_{rabc}] \} \\ [v_{rabc}] &= [R_r][i_{rabc}] + \frac{d}{dt} \{ [L_r][i_{rabc}] + [M_{sr}][i_{sabc}] \} \end{aligned} \quad (\text{II.36})$$

The couple will be given by:

$$T_e = p [i_{sa} \ i_{sb} \ i_{sc}] \frac{d}{d\theta} [M_s] \begin{bmatrix} i_{ra} \\ i_{rb} \\ i_{rc} \end{bmatrix} \quad (\text{II.37})$$

II.6.3 IM speed selector

The choice of the speed of the IM is limited by the fact that the synchronous speed is determined only by the frequency of the network and by the number of poles of the machine. Therefore, with a 60 Hz power source, it is impossible to design an IM with both an acceptable efficiency and a speed of, for example, 2000 rpm. Such a motor would necessarily have two poles, but with a synchronous speed of 3600 rpm, the slip would be $(3600 - 2000) / 3600 = 0.44$. This means that 44% of the power supplied to the rotor would be dissipated in the form of heat, resulting in very poor efficiency.

For a specific application, the choice of motor speed is determined by the nature of the load to be driven. When it comes to low-speed loads, it is often more advantageous to use a high-speed motor with a speed reducer (gear, pulley) rather than a low-speed motor coupled directly to the load. The advantages of an engine with a gearbox are:

- For a given power, the size and cost of a high-speed engine are smaller than a low-speed engine;
- The efficiency and power factor of the asynchronous motors is the higher the speed;
- The relative starting torque (in units per power) of a high-speed engine is always higher than that of a low-speed engine of the same class.

II.6.4 Equation of the IM

A) Electrical equations

The behavior of the machine can be translated into three types of phenomena governed by their respective equations: electric equation; magnetic and mechanical [16].

Be (V_{sabc}) , (i_{sabc}) and (Φ_{sabc}) , respectively, the voltage, current and flux vector of the three stator phases of the machine

$$[V_{sabc}] = \begin{bmatrix} V_{sa} \\ V_{sb} \\ V_{sc} \end{bmatrix}; [I_{sabc}] = \begin{bmatrix} I_{sa} \\ I_{sb} \\ I_{sc} \end{bmatrix}; [\varphi_{sabc}] = \begin{bmatrix} \varphi_{sa} \\ \varphi_{sb} \\ \varphi_{sc} \end{bmatrix} \quad (\text{II.38})$$

The same ratings are adopted for the rotoric quantities by replacing the 's' index with the 'r' index. The stator and rotoric voltages are defined as follows:

• Stator phase

For all stator windings, matrix notations will be written:

$$\begin{bmatrix} V_{sa} \\ V_{sb} \\ V_{sc} \end{bmatrix} = \begin{bmatrix} R_s & 0 & 0 \\ 0 & R_s & 0 \\ 0 & 0 & R_s \end{bmatrix} \cdot \begin{bmatrix} I_{sa} \\ I_{sb} \\ I_{sc} \end{bmatrix} + \frac{d}{dt} \begin{bmatrix} \varphi_{sa} \\ \varphi_{sb} \\ \varphi_{sc} \end{bmatrix} \quad (\text{II.39})$$

With:

R_s : Stator phase resistance.

• Rotor phase

For all rotoric windings, matrix notation will read:

$$\begin{bmatrix} V_{ra} \\ V_{rb} \\ V_{rc} \end{bmatrix} = \begin{bmatrix} R_r & 0 & 0 \\ 0 & R_r & 0 \\ 0 & 0 & R_r \end{bmatrix} \cdot \begin{bmatrix} I_{ra} \\ I_{rb} \\ I_{rc} \end{bmatrix} + \frac{d}{dt} \begin{bmatrix} \varphi_{ra} \\ \varphi_{rb} \\ \varphi_{rc} \end{bmatrix} \quad (\text{II.40})$$

R_r : Rotor phase resistance.

B) Magnetic equations

The hypotheses mentioned above, lead to the following relations between the flows (φ) and the currents (i) of the statoric and rotoric phases

$$\begin{bmatrix} \varphi_{sabc} \\ \varphi_{rabc} \end{bmatrix} = \begin{bmatrix} [L_s] & [M_{rs}] \\ [M_{rs}] & [L_r] \end{bmatrix} \cdot \begin{bmatrix} I_{sabc} \\ I_{rabc} \end{bmatrix} \quad (\text{II.41})$$

With

$$[L_s] = \begin{bmatrix} L_{as} & M_s & M_s \\ M_s & L_{as} & M_s \\ M_s & M_s & L_{as} \end{bmatrix} \quad (\text{II.42})$$

$$[L_r] = \begin{bmatrix} L_{ar} & M_r & M_r \\ M_r & L_{ar} & M_r \\ M_r & M_r & L_{ar} \end{bmatrix} \quad (\text{II.43})$$

The mutual inductors stator-rotor depend on the angle α (position of the rotor) and have the value to peak M_{sr} .

$$[M_{sr}] = [M_{rs}]^t = \begin{bmatrix} M_1 & M_3 & M_2 \\ M_2 & M_1 & M_3 \\ M_3 & M_2 & M_1 \end{bmatrix} \quad (\text{II.44})$$

$$\begin{bmatrix} \varphi_{sa} \\ \varphi_{sb} \end{bmatrix} = \begin{bmatrix} L_{as} & M_s & M_s & M_1 & M_3 & M_2 \\ M_s & L_{as} & M_s & M_2 & M_1 & M_3 \end{bmatrix} \cdot \begin{bmatrix} I_{sa} \\ I_{sb} \end{bmatrix} \quad (\text{II.45})$$

Finally, the magnetic equations in matrix form of the statoriq and rotoric phases will be as follows:

$$\begin{bmatrix} \varphi_{sc} \\ \varphi_{ra} \end{bmatrix} = \begin{bmatrix} M_s & M_s & L_{as} & M_3 & M_2 & M_1 \\ M_1 & M_2 & M_3 & L_{ar} & M_r & M_r \end{bmatrix} \cdot \begin{bmatrix} I_{sc} \\ I_{ra} \end{bmatrix} \quad (\text{II.46})$$

$$\begin{bmatrix} \varphi_{rb} \\ \varphi_{rc} \end{bmatrix} = \begin{bmatrix} M_3 & M_1 & M_2 & M_r & L_{ar} & M_r \\ M_2 & M_3 & M_1 & M_r & M_r & L_{ar} \end{bmatrix} \cdot \begin{bmatrix} I_{rb} \\ I_{rc} \end{bmatrix} \quad (\text{II.47})$$

With

L_{as} : Clean inductance of a stator phase.

L_{ar} : Clean inductance of a rotor phase.

M_s : Mutual inductance of a stator phase.

M_r : Mutual inductance of a rotor phase.

M_{sr} : Maximum mutual inductance between two stator and rotor phases.

From the previous relations the electrical equations become:

$$[V_{sabc}] = [R_s] \cdot [I_{sabc}] + \frac{d}{dt} \{ [L_s][I_{sabc}] + [M_{sr}][I_{rabc}] \} \quad (\text{II.48})$$

$$[V_{rabc}] = [R_r] \cdot [I_{rabc}] + \frac{d}{dt} \{ [M_{rs}][I_{sabc}] + [L_r][I_{rabc}] \} \quad (\text{II.49})$$

C) Mechanical equation

The mechanical equation governing the speed of rotation of the machine is given by

$$J \frac{d}{dt} \omega = T_{em} - CT_r - f\omega \quad (\text{II.50})$$

With:

J: Moment of inertia brought back on the machine shaft.

T_{em} : Electromagnetic torque developed by the machine.

T_r : Load resistant torque.

F: Viscous coefficient of friction.

The electromagnetic torque is the partial derivative of the magnetic coenergy relative to the position. Knowing that eigenvectors are null derivatives, there remains only the term relative to derivatives of mutual inductances. Its expression is given by:

$$T_{em} = \frac{1}{2} P [I_{sabc}^t] \cdot \frac{\partial}{\partial \theta} [M_{sr}] [I_{rabc}] \quad (\text{II.51})$$

With:

P: is the number of pairs of poles

II.7 Centrifugal pumps

A centrifugal pump is an open system, similar to a hole or conduit, in which a field of centrifugal forces is established. Unlike a bucket or a volume of imprisonment, the centrifugal pump does not rely on fluid transport or temporal variations, but rather on the movement and balancing of the fluid by a force field. Although this concept is very simple, it is based on other principles, as we will see later. The centrifugal pump works and is used

according to other laws, which will be discussed in the following paragraphs. Although we covered the essentials, some narrow areas or specific aspects were not addressed.

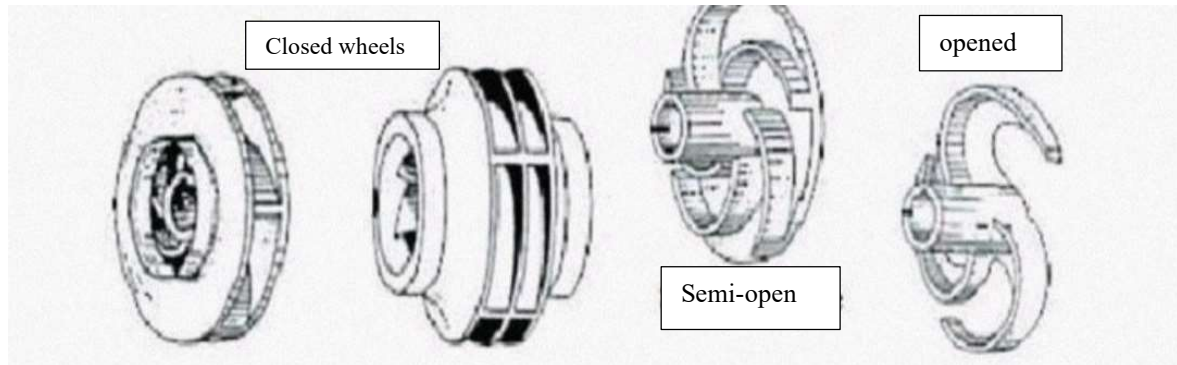


Fig II.25 centrifugal pump

II.7.1 Using of Centrifugal pumps

Centrifugal pumps are widely used in the industry because of their versatility, simplicity, and affordability. However, there are applications for which they are not suitable, such as pumping viscous liquids, which would require a centrifugal pump of enormous size compared to other possible flows. In addition, "sensitive" liquids that do not support excessive agitation in the pump (such as food liquids such as milk) are not suitable for use with centrifugal pumps. Similarly, for applications requiring precise and instantaneous dosing, it is risky to use a centrifugal pump because it could make it work outside its optimal characteristics. For these types of applications, positive displacement pumps are preferred. However, unlike most positive displacement pumps, centrifugal pumps can handle suspensions loaded with solids.

II.7.2. Operation of Centrifugal pumps

The circular suction flange B_1 evenly distributes the fluid to the inlet section C of the moving channels called the "suction hearing" of the pump. The area between B_1 and C is called the suction bottom and represents the seat of continuous flow due to the drive movement at constant angular velocity.

The pump stator S , also known as the body or casing, has a fixed vane crown F called a "fixed fin diffuser," which is symmetrical to the axis. Each space between two fixed blades constitutes a fixed channel. The energy received by the fluid during its passage through the mobile channels results in an increase in its pressure and kinetic energy. Part of this kinetic energy is converted into pressure in the fixed blades at the outlet of the diffuser.

The fluid must then be collected and directed to the T_2 piping. This function is fulfilled by a V capacity that wraps around the diffuser and is called volute because of its geometric shape. This volute is used to transform part of the kinetic energy into pressure energy.

The blades exert pressure on the fluid, creating an overpressure along their outer side and a depression on their inner side.

The impellers of centrifugal pumps are often closed, consisting of two flanges spaced by the blades. These blades can be semi-open with a single rear flange or open without a flange. All these centrifugal wheels are fed axially by the liquid. After circulation through the channels, the liquid exits radially from the axis of rotation.

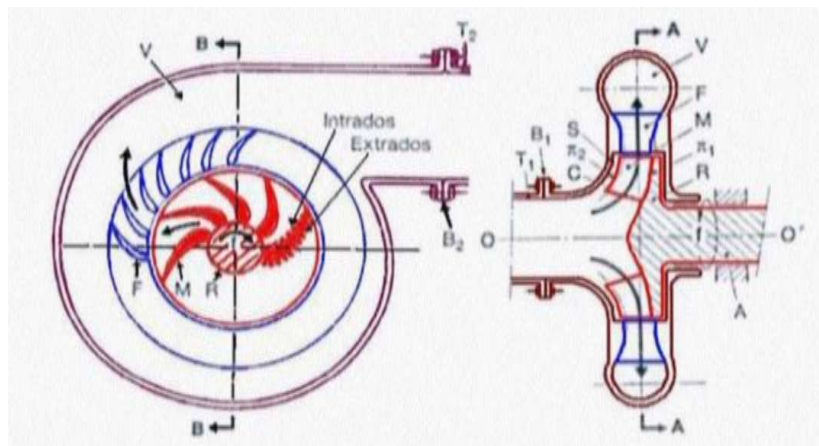


Fig II.26 Working principle of centrifugal pump

II.7.3 The mathematical model of centrifugal pump

II.7.3.1 Hydraulic model

The hydraulic model of a centrifugal pump can be described by the following equations:

Equation of the total manometric height

$$H = H_s + H_f + H_v \quad (\text{II.52})$$

H_s : static

H_c : kinetic

H_v : frictio

a. Static height equation:

$$H_s = \frac{P_2 - P_1}{\rho g} \quad (\text{II.53})$$

b. Kinetic height equation:

$$H_c = \frac{V^2 - V_1^2}{2g} \quad (\text{II.54})$$

c. Friction Height Equation:

$$H_v = \frac{fL}{2g} \quad (\text{II.55})$$

Where:

- H is the total manometric height.
- static H_s is the static height.
- kinetic H_c is the kinetic height.
- friction H_v is the friction height.

- P_1 and P_2 are the pump inlet and outlet pressures.
- ρ is the density of the fluid.
- g is acceleration due to gravity.
- V_1 and V_2 are the fluid speeds at the pump inlet and outlet.
- f is the coefficient of pressure loss.
- L is the length of the pipe.
- D is the diameter of the pipe.

II.7.3.2 Mechanical model

The mechanical model of a centrifugal pump can be described by the following equations:

a) Hydraulic Power Equation:

$$P_h = \rho * g * Q * H \quad (\text{II.56})$$

b) Mechanical Power Equation:

$$P_m = \tau * \omega \quad (\text{II.57})$$

Where:

- P_h is the hydraulic power supplied by the pump.
- P_m is the mechanical power provided by the engine.
- Q is the volumetric flow of the fluid.
- H is the total manometric height.
- ρ is the density of the fluid.
- g is acceleration due to gravity.
- τ is the mechanical torque applied to the pump shaft.
- ω is the angular velocity of the pump shaft.

By combining these hydraulic and mechanical equations, it is possible to model the complete behavior of a centrifugal pump under different operating conditions.

II.8 Conclusion

In this chapter we have studied the modelling of different elements of photovoltaic pumping system: such as photovoltaic system, converters: chopper, inverter, asynchronous machine and centrifugal pump.

Chapter III: Design and Simulation of the Photovoltaic Pumping System

III. 1 Introduction

In this last chapter, we will describe an autonomous photovoltaic water pumping system driven by an induction motor without energy storage in order to improve performance. We will apply to the system the "Disturb and Observe" (P&O) method, which ensures high efficiency when monitoring the maximum power point of the photovoltaic panel in case of sudden variations in sunlight. This MPPT acts on the cyclic ratio of the elevator converter. The latter combines with a voltage source inverter to convert DC to AC to drive the three-phase induction motor that runs the centrifugal pump. The simulation results of this work will be obtained in the MATLAB Simulink environment.

In the second part, we will present the method of sizing a photovoltaic pumping system to meet the water needs of a given consumption. This method is essentially based on the assessment of water needs, the calculation of the necessary hydraulic energy, the determination of the available solar energy and the choice of appropriate components.

III. 2 Sizing of a photovoltaic pumping system

In this part we will design a photovoltaic pumping system, with an acceptable degree of precision. The most important factors of this approach will have to be carefully estimated in order to obtain a satisfactory sizing

III.2.1 Sizing of the photovoltaic field

III.2.1.1 Determination of available solar energy

The sizing method used is based on the calculations of the monthly average daily values of the available solar irradiation and the necessary hydraulic energy.

a- Photovoltaic generator tilt

The inclination β of photovoltaic (PV) modules to the horizontal plane must be done in such a way as to optimize the ratio between solar irradiation and the necessary hydraulic energy.

b- Month of design

The month of dimensioning will be the most unfavorable month, that is, the one whose ratio between solar irradiation and the necessary hydraulic energy is minimal. As an idea of principle, each inclination β corresponds to the most unfavorable month. The month of design at the optimal inclination will be precisely the one with the smallest ratio between solar irradiation and hydraulic energy. The solar irradiation and the corresponding hydraulic energy required for this month will be used for the selection of system components [17].

c- Assessment of the average daily energy required by the load [18]

The average consumption required for the operation of equipment in (Wh/d) is given by the following formula:

$$C_j = \sum P h \quad (III.4)$$

With:

P: The electrical power consumed by the load (in W).
Average Daily Use Time (I_n).

a- Estimation of the number of modules in series

The number of modules in series is:

$$N_s = U U_n \quad (III.5)$$

U: Installation voltage in V.

U_n : Nominal voltage of a V-module.

b- Estimation of the number of branches in parallel

$$N_p = N N_s \quad (III.6)$$

N_s : Number of modules in parallel.

N: Number of modules.

a- Generator Power Calculation

The peak power delivered by the generator is:

$$P_s = N_s \cdot P_s \cdot P_{cm} \quad (III.7)$$

P_{cm} : Peak power of a module.

P_s : Peak power of a generator.

b-Calculation of the total area of the generator

The total area occupied by the field on the ground or you is:

$$S = N \cdot S_m \quad (III.8)$$

S_m : C'est la surface d'un module en m^2 .

N : Nombre de module.

III.2.2 Engine sizing

The motor uses are a three-phase cage asynchronous motor, with a power of 3.5KW. The chosen engine must be able to withstand the peak power of the photovoltaic generator.

III.2.3 Dimensioning of the centrifugal pump

The peak flow rate [m^3/h] is calculated by the following relationship [32]:

$$Q = \frac{3.6 ph}{g.h} \quad (III.9)$$

Where:

ph: Hydraulic power required [W].

g: Acceleration of gravity [$9.81m/s^2$].

h: Total gauge height[m].

III.3 Direct torque control technology DTC

The direct torque control (DTC) technique appeared in the second half of the 1980s as competitive with conventional methods, based on a pulse width modulated power supply (MLI) and on a decoupling of flux and torque by the orientation of the magnetic flux [19]. DTC is a control technique that ensures a decoupling of flow and torque and is simple to implement. It has already well-known advantages over conventional techniques, particularly in terms of reducing torque response time, improving its robustness compared to variations in rotoric parameters, the direct imposition of the amplitude of the torque ripples and the stator flux, and the absence of Park transformations. On the other hand, this law of torque control adapts by nature to the absence of mechanical sensors (speed and position). Much work has been done by researchers in this field, whose goal is to improve the basic technique stated by Takahash.

III.3.1 Principle of direct torque control

Direct torque control is based on the direct determination of the control sequence to be applied to a voltage inverter. This choice is generally based on the use of hysteresis regulators, whose function is to control the state of the system, namely the amplitude of the stator flow and the electromagnetic torque. [20], [21] The state of these quantities allows us to define the stator voltage vector to be applied to the asynchronous machine to best maintain the torque to the flow in their hysteresis bands. A variable also involved in the choice of voltages is the position of the stator vector in the complex plane. For this, the plan is divided into six sectors and sometimes twelve. The block diagram of this technique is shown in the following (Fig III.1). In this figure, the flow and torque estimators, as well as the regulators, are represented by the hysteresis of the torque and flow. The position of the flow vector is calculated from its components in the complex $\alpha\beta$ plane. The flow regulator is at two levels, and the three-level torque regulator was initially proposed by Takahashi [21].

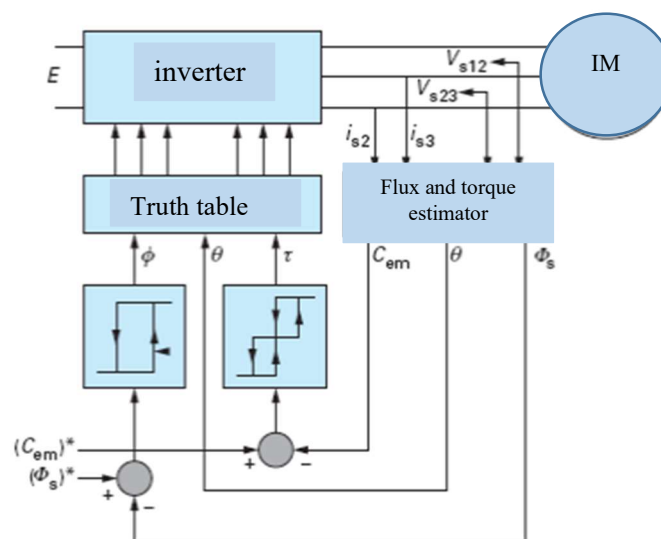


Fig III.1 DTC structure diagram applied to an IM

III.3.2 Flow and torque control

III.3.2.1 Flow Control

One stands in a fixed $\alpha\beta$ bound to the stator of the machine. The stator flow can be obtained by the following equation:

$$\overline{R}_s = R_s \overline{I}_s + \frac{d\overline{\varphi}_s}{dt} \Rightarrow \overline{\varphi}_s = \overline{\varphi}_{s0} + \int_0^t (\overline{V}_s - R_s \overline{I}_s) dt \quad (III.1)$$

Si on néglige la chute de tension due à la résistance l'équation (III.1) devient :

$$\overline{\varphi}(K+1) \approx \overline{\varphi}(k) + \overline{V}_s T_e \Rightarrow \Delta \overline{\varphi}_s \approx \overline{V}_s T_e \quad (III.2)$$

Où :

- $\overline{\varphi}(k)$: stator flow vector at current sampling step
- $\overline{\varphi}(k+1)$: stator flow vector at the following sampling step
- T_e : sampling period

We find that the end of the stator flow vector describes, from its initial state, a line parallel to the applied voltage vector (see Fig III.2). [19]

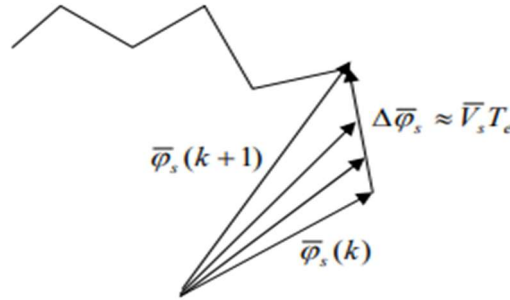


Fig III.2 Evolution of the flux vector in the $\alpha\beta$ plane

The relation (III.2) shows that the speed of rotation of the flow is equal to the applied voltage. The application of a vector colinear tension with the vector flux acts directly on the amplitude of the latter. On the other hand, if we apply a voltage vector quadrature with the flow, it acts on the phase of the flow and causes either an acceleration or a deceleration of the flow vector. Finally, if we apply a zero voltage (V_0 or V_7), the flow vector remains fixed.

III.3.2.2 Torque Control

The electromagnetic torque is proportional to the vector product of the two stator and rotor flows.

$$T_e = K(\overline{\varphi}_s \wedge \overline{\varphi}_r) = K|\overline{\varphi}_s||\overline{\varphi}_r|\sin(\theta) \quad (III.3)$$

The angle θ is the phase shift between the two flows. The stator flow is the sum of the rotor flow and the total leakage flow. The dynamics of these two components are not the same: [21], [19]

- Leak flow has rapid dynamics due to voltage variations as leakage inductances are low

- The rotational flux, dependent on the magnetizing inductance, has a slower dynamics, about ten times slower in reference to the coefficient of dispersion σ whose average value is about 0.1.

Under these conditions, it can be assumed that between two switches, the rotor flow remains constant. On the other hand, the stator flow is directly affected by variations in leakage flows. So the torque depends only on the product $\sin \phi_s$.

Since the amplitude of the stator flux varies relatively little, the torque variation can be achieved by variation of the angle θ .

III.3.3 Direct Torque Control Strategy

Direct torque control is based on the following algorithm:[21], [20]

- The time domain is divided into T_e duration periods ($T_e 50\mu s$)
- At each clock stroke, line currents and voltages are measured
- Reconstruct the stator flow vector components
- The couple is estimated by the following relationship: $T_e = p(\phi_{s\alpha} I_{s\beta} - \phi_{s\beta} I_{s\alpha})$
- The tension vector to be applied to the machine is determined according to a logic which will be presented in the following
- The control synoptic of this strategy is presented in the following figure:

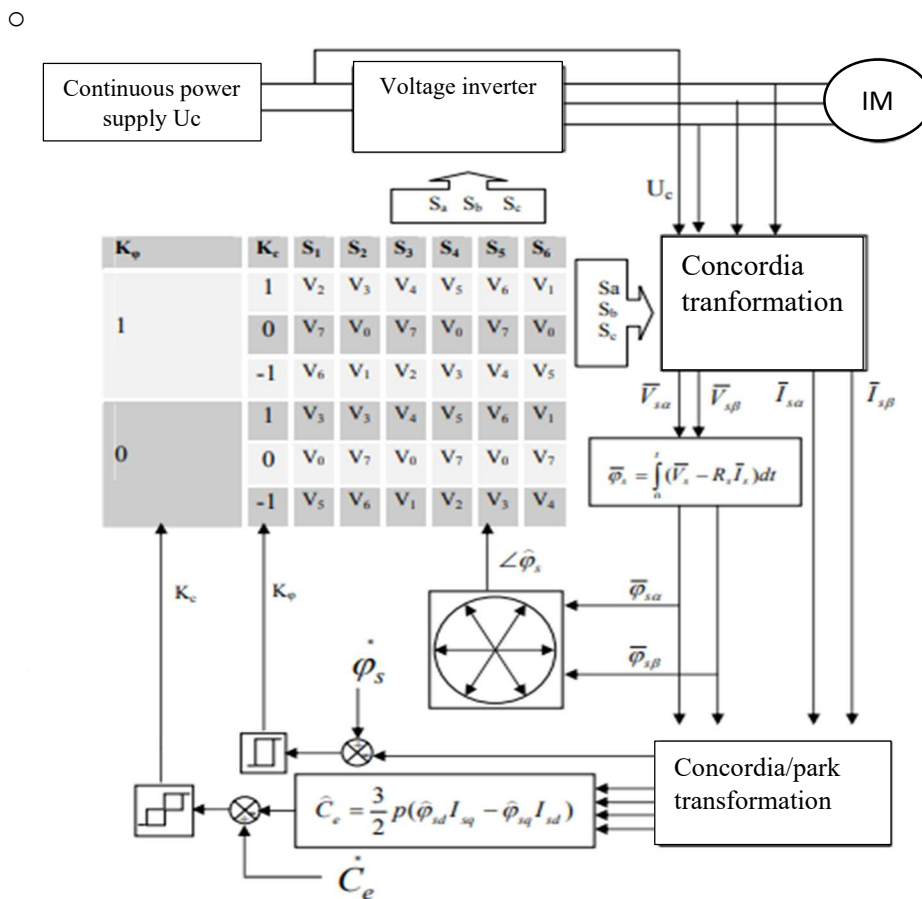


Fig III.3 DTC control block diagram

III.3.4 Estimators

III.3.4.1 Stator flow estimator

The estimation of the flow can be made from the measurements of the current stator quantities and machine voltage. From equation:

$$\overline{\varphi}_s = \int_0^t (\overline{V}_s - R_s \overline{I}_s) dt \quad (III.4)$$

The α and β components of vector ϕ_s are obtained

$$\varphi_{s\alpha} = \int_0^t (V_{s\alpha} - R_s I_{s\alpha}) dt \quad (III.5)$$

$$\varphi_{s\beta} = \int_0^t (V_{s\beta} - R_s I_{s\beta}) dt \quad (III.6)$$

The voltages $V_{s\alpha}$ and $V_{s\beta}$ are obtained from the commands (S_a S_b S_c) and the measurement of the voltage U_d and by application of the Concordia transformation :

$$\overline{V}_s = V_{s\alpha} + jV_{s\beta} \quad (III.7)$$

$$V_{s\alpha} = \sqrt{\frac{2}{3}} U_d (S_a - \frac{1}{2} (S_b + S_c)) \quad (III.8)$$

$$V_{s\beta} = \frac{1}{\sqrt{2}} U_d (S_b - S_c) \quad (III.9)$$

Similarly the currents are obtained from the measurement of real currents, I_{sa} , I_{sb} , I_{sc} and by applying the Concordia transform:

$$\begin{cases} \overline{I}_s = I_{s\alpha} + jI_{s\beta} \\ I_{s\alpha} = \sqrt{\frac{2}{3}} I_{sa} \\ I_{s\beta} = \frac{1}{\sqrt{2}} (I_{sb} - I_{sc}) \end{cases} \quad (III.10)$$

The stator flow module is written:t :

$$\varphi_s = \sqrt{\varphi_{s\alpha}^2 + \varphi_{s\beta}^2} \quad (III.11)$$

The zone Ni in which the vector ϕ_s is located is determined by the calculation of the phase of the vector :

$$\angle \overline{\varphi}_s = \arctg \frac{\varphi_{s\alpha}}{\varphi_{s\beta}} \quad (III.12)$$

III.3.4.2 Estimation of electromagnetic cutting

The couple can be estimated from the following relation ship :

$$T_e = \frac{3}{2} p (\widehat{\varphi}_{s\alpha} I_{s\beta} - \widehat{\varphi}_{s\beta} I_{s\alpha}) \quad (III.13)$$

III.3.5 Correctors

III.3.5.1 Flow Corrector

The purpose of this correction is to preserve the amplitude of the stator flow in a band and thus maintain the end of the latter in a circular crown. [19], [20]

The output of the corrector must indicate the direction of evolution of the flow module. The two thresholds of the comparator are chosen according to the wave tolerated by the stator flow. One can then write:

$$\left\{ \begin{array}{ll} \text{if } \Delta\varphi_s > \varepsilon_\varphi & \text{then } K_\varphi = 1 \\ \text{if } 0 \leq \Delta\varphi_s \leq \varepsilon_\varphi \text{ et } \frac{d\Delta\varphi_s}{dt} > 0 & \text{then } K_\varphi = 0 \\ \text{if } \Delta\varphi_s \leq -\varepsilon_\varphi \text{ et } \frac{d\Delta\varphi_s}{dt} < 0 & \text{then } K_\varphi = 1 \\ \text{if } -\varepsilon_\varphi < \Delta\varphi_s < 0 & \text{then } K_\varphi = 0 \end{array} \right. \quad (\text{III.14})$$

$K_\varphi=0$ means to reduce the flow.

$K_\varphi=1$ means to increase the flow.

This two-level hysteresis regulator is perfect for having good dynamic performance.

III.3.6 Torque Corrector

The purpose of the torque corrector is to keep the torque in its hysteresis band and thus impose the amplitude of the torque ripples. To better control the torque in the four operating dials without intervention on the structure; Takahashi proposed a three-level hysteresis corrector. [21] This corrector allows control of the machine in both directions of rotation with positive or negative torque.

III.3.6 Choise of voltage vector

The choice of the stator tension vector V_s depends on the position of the stator flux vector in the complex plane $\alpha\beta$, the desired variation for the modulus of the flux ϕ_s , the desired variation for the torque, and the direction of rotation of the flux. [19], [21], [22] The flow evolution space is divided into six zones called sectors, as shown in (Fig III.4). • When the ϕ_s flow is in an i -zone, flow and torque control can be achieved by selecting one of the following six vectors:

- If V_{i+1} is selected then ϕ_s believes and believes this
- If V_{i-1} is selected then ϕ_s believes and decreases this
- If V_{i+2} is selected then decreases and increases
- If V_{i-2} is selected then ϕ_s decreases and decreases this
- If V_0 or V_7 is selected the rotation of ϕ_s is stopped, hence a decrease in torque while the torque module remains unchanged.

The efficiency level of the applied tension vectors also depends on the position of the flow vector in zone i . Indeed, at the beginning of the zone, the vectors V_{i+1} and V_{i-2} are perpendicular to ϕ_s , hence a rapid evolution of the torque but a slow evolution of the amplitude of the flow, while at the end of the zone, the evolution is inverse. With vectors V_{i-1} and V_{i+2} , it corresponds to a slow and rapid evolution of the torque and amplitude of ϕ_s at the beginning of the zone, while at the end of the zone it is the opposite. Regardless of the direction of flux or torque evolution, in zone i , the two vectors V_i and V_{i+3} are never used.

Indeed, these two vectors cause a strong growth of the flow, but its effect on the couple depends on the zone, with a zero effect in the middle of the zone. The stator voltage vector V_s at the output of the inverter is deduced from the estimated torque and flow deviations from their references, as well as from the position of the vector. A module, a position ϕ_s estimator, and a torque estimator are therefore required.

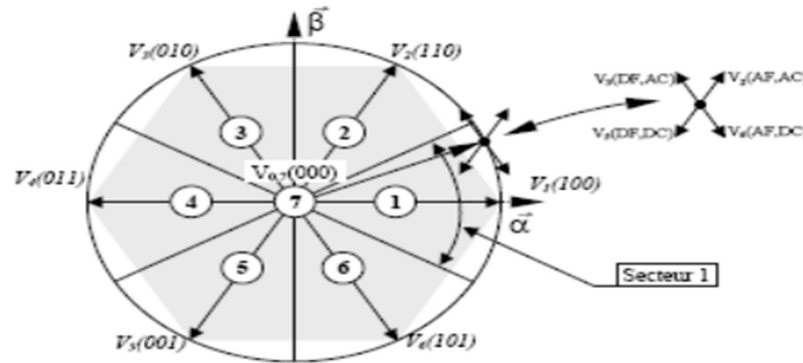


Fig III.4 starting from the complex plan in six sectors

III.3.7 Elaboration of the switching tables

III.3.7.1 Switch table with null sequences

The switching table is constructed from the behavior of the system given by the variables K_ϕ and K_c and the stator flow sector. The evolution of the two flow and torque quantities for each of the four vectors $V_{i+1}, V_{i+2}, V_{i-1}, V_{i-2}$ which can be applied to the asynchronous machine in the sector S_i is shown in the following table :

Table III.1 Table for the choice of tension vectors

	V_{i+1}	V_{i+2}	V_{i-1}	V_{i-2}
ϕ_s	↗	↘	↗	↘
T_e	↗	↗	↘	↘

To explain how to build the switching table, we consider the example where $K_\phi = 1, K_c = 1,$ and $S_i = 1$. The flow vector is in sector 1, and you have to increase the torque and the flow. You have the six active voltages. We see that the voltages $V_1, V_2,$ and V_6 tend to increase the amplitude of the flow, while $V_2, V_3,$ and V_4 tend to accelerate the flow vector, thus increasing the angle θ and therefore the torque. We verify that for this position of the flow vector in sector 1, only the voltage V_2 is able to increase both the amplitude of the flow and the torque. So you can look at different cases. We choose a zero sequence whenever $K_c = 0,$ that is, when the couple is inside its band of hysteresis. The choice between V_0 and V_7 is made to reduce the frequency.

Table III.2 switching tabla defined by takahashi

K_ϕ	K_c	S_1	S_2	S_3	S_4	S_5	S_6
1	1	V ₂	V ₃	V ₄	V ₅	V ₆	V ₁
	0	V ₇	V ₀	V ₇	V ₀	V ₇	V ₀
	-1	V ₆	V ₁	V ₂	V ₃	V ₄	V ₅
0	1	V ₃	V ₄	V ₅	V ₆	V ₁	V ₂
	0	V ₀	V ₇	V ₀	V ₇	V ₀	V ₇
	-1	V ₅	V ₆	V ₁	V ₂	V ₃	V ₄

III.3.7.2 Table de commutation sans séquences nulles

switching. Based on these assumptions, we can establish the switching table proposed by Takahashi. [19], [21], [22], [20] We notice that we move from one sector to the next by a circular permutation of the voltage index.

III.3.8 The advantages and disadvantages

Direct torque control has the following advantages (compared to vector control).

- Torque and flow can be changed quickly by changing their setpoint respective.
- Good performance with transistors switched only when needed.
- Response at a level not exceeded.
- No Park Transform so no need to know position of the rotor to calculate the algorithm.
- Modulation is performed directly by the method.
- No integrative proportional controller (PI)
- Due to hysteresis control, the switching frequency is not constant. However, setting the tolerance range allows the average switching frequency to be adjusted approximately
- .• No peak current. Direct torque control has the following disadvantages
- .• The controller must be very fast. It needs a lot of computing power. In effect, the algorithm should be calculated very regularly, approximately every 10 to 30 μ s, to prevent the flow or the couple from going out of tolerance. In On the other hand, the algorithm is relatively simple.
- The current sensor must be of very good quality, so as not to mislead the controller. A low-pass filter cannot be inserted into the circuit to remove noise. The delay it would cause would prevent the proper functioning of hysteresis.

- The voltage measurement must also be of good quality, for reasons similar. In general, an estimation of the stator voltage from the DC voltage of intermediate circuit and control signal transistors are used.
- In high speed, the method is not sensitive to engine parameters. This is not the case in low speed, where stator resistance plays a role important in estimating the flow.

III.4 The MPPT command

An MPPT (Maximum Power Point Tracker) is a principle allowing to follow, as its name suggests, the maximum power point of a non-linear electric generator. MPPT systems are generally associated with photovoltaic generators or with wind generators [23].

By definition, an MPPT control, associated with an intermediate stage of adaptation, allows for the operation of a generator P+V in order to continuously produce the maximum of its power. Thus, whatever the weather conditions (temperature and illumination), the converter control places the system at the maximum operating point (V_{mpp} , I_{mpp}). Impedance adaptation is often in the form of a DC-DC converter, as shown in (Fig III.5). [24]

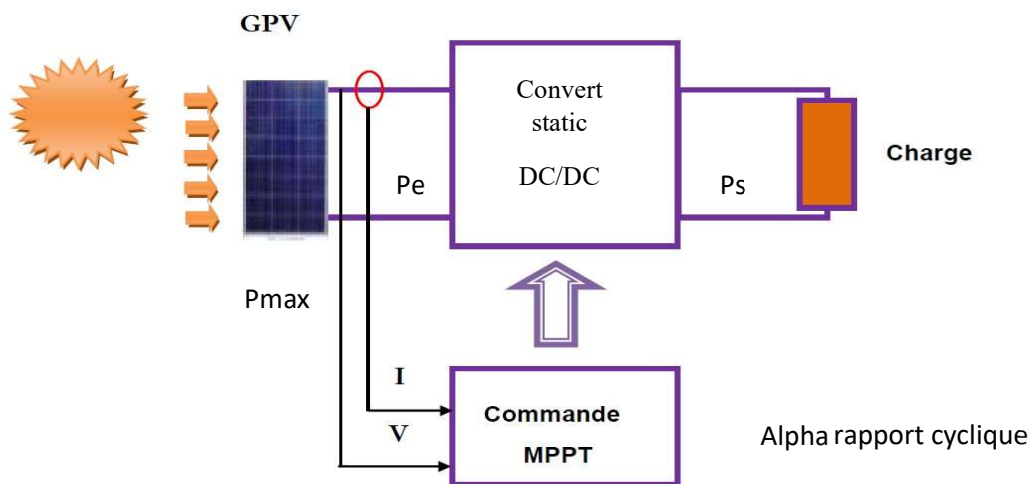


Fig III.5 Solar power conversion chain including MPPT control

III.4.1 The main features and functionality

The following are the main features and functionality of an MPPT command:

- MPPT Algorithm: This is the heart of the device. It implements a PPM tracking algorithm by continuously adjusting the operating voltage of solar panels to maximize the power output. The most common algorithms are disturbance and observation, and incremental conductance.
- DC-DC conversion: The MPPT control incorporates a DC-DC converter that adapts the panel voltage (variable according to the PPM) to the battery or DC bus voltage for optimal power transfer.

- PV Input: Connects the solar panels to the control. The maximum allowable input voltage varies by model (typically 100-150V).
- Battery Output: This is the connection to the system's battery or DC bus. The MPPT control optimally regulates the load current and voltage.
- Display and control: An LCD screen or a communication port allows to view the data (voltages, currents, power) and to adjust the charging parameters. Protections: Against surges, short circuit, reverse polarities, extreme temperatures, etc.
- High efficiency: Up to 98% efficiency to transfer power from panels to load.

III.4.2 The methods of the MPPT command

The main methods used by MPPT controls to track the maximum power point of the solar panels:

. Disturbance and Observation (P&O) Method:

- Periodically disrupts operating voltage and observes effect on power
- Simple to implement but may have oscillations

. Incremental Conductance Method:

- Uses power derivatives versus voltage
- Converges faster with fewer oscillations but more complex

. Constant Voltage Method:

- Adjusts the operating voltage to a fixed percentage of the open circuit voltage
- Simple but less precise, especially in case of temperature changes

. Power Curve Method:

- Analytically models the panel power curve
- Precise but complex to implement, requires detailed modelling

The choice of the method depends on a trade-off between tracking accuracy, speed of convergence, computational complexity and available hardware resources in the MPPT controller. The P&O and Incremental Conductance methods are the most widespread.

III.4.3 The Perturbation & Observation (P&O) method

The perturbation and observation method is a widely used approach in the search for the maximum power point (MPPT) because it is simple and easy to achieve. P&O works with the V_{pV} voltage disturbance, and observing the impact of this change on the PV panel output power as shown in the figures represents the P&O method algorithm. At each cycle, the voltage V_{pv} and the current I_{pv} are measured to calculate (k) . This value of (k) is compared to the value $P_{(k+1)}$ calculated in the previous cycle.

If the output power has increased, V_{pv} is adjusted in the same direction as in the previous cycle. If the output power has decreased, V_{pv} is adjusted in the opposite direction than in the previous cycle. V_{pv} is thus disturbed at each MPPT cycle. When the maximum power point is reached, V_{pv} oscillates around the optimal VPPM value. This causes a power loss that increases with the step of the disturbance increment.

If this increment step is wide, the MPPT algorithm responds quickly to rapid changes in operating conditions. It is therefore necessary to find a compromise between precision and speed. Another disadvantage of the P&O method is that it can fail and misinterprets the location of the MPP during a rapid change in atmospheric conditions.

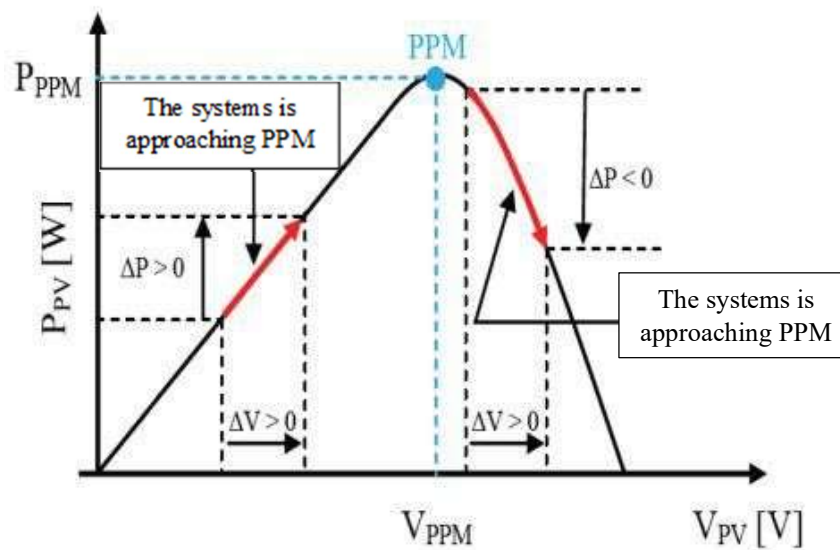


Fig III.6 Block diagram of the P&O method

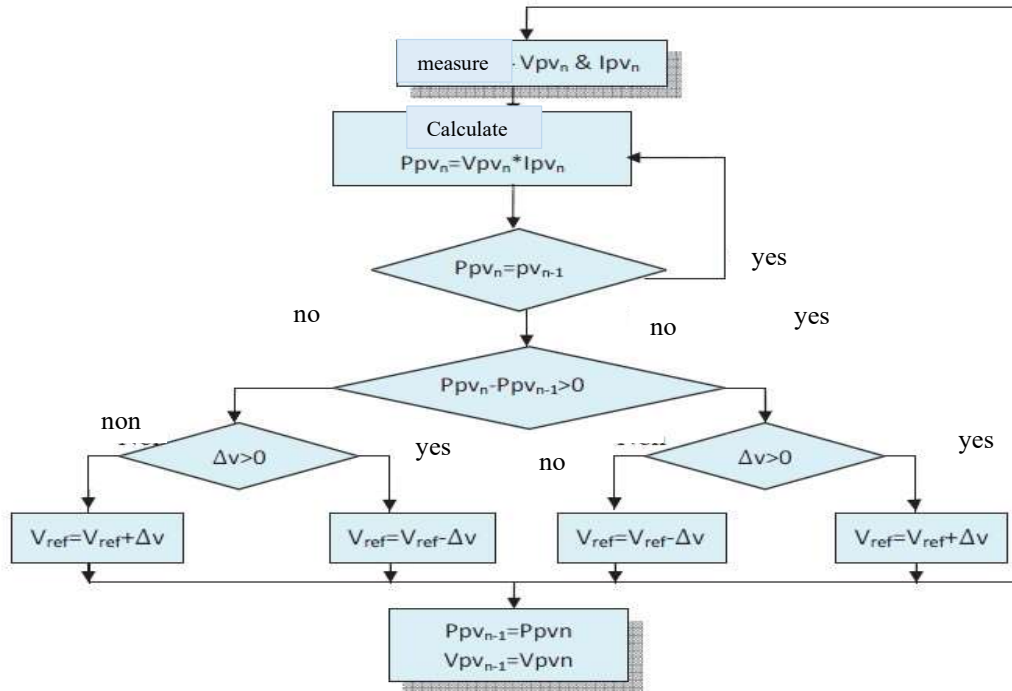


Fig III.7 Perturbation and observation method algorithm

III.5 Simulation and results

Results of the Simulation of a Photovoltaic Pumping System we simulated the photovoltaic pumping system, which consists of a photovoltaic generator composed of two solar panels in parallel with a BOOST chopper controlled by Maximum Power Point Tracking (MPPT) classic, which is Perturb and Observe (P&O). An inverter that converts the continuous voltage delivered by the PV system. The load consists of a motor-pump (alternating-current motor and centrifugal pump). The simulation is performed under climatic conditions: variable brightness and constant temperature ($T = 25\text{ }^{\circ}\text{C}$).

Temperature influence : respectively represent the influence of temperature on the current-voltage and power-voltage characteristics of the $1000\text{W}/\text{m}^2$ constant illumination PV generator. The current increases slightly as the temperature increases, but the temperature negatively affects the voltage. As a result the maximum power decreases with temperature.

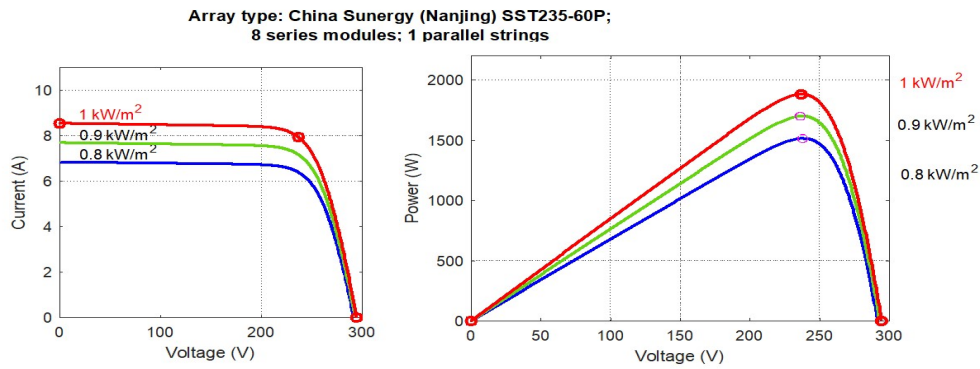


Fig III.8 Curve of variation of currant and power as a function of time

Influence of irradiation : represent the influence of illumination on the current-voltage and power-voltage characteristics of the PV generator. At a constant temperature of 25°C, the current changes significantly, but the voltage varies slightly. As for the maximum power of a photovoltaic generator, when the illumination is higher, the GPV generates more power. The standard, internationally accepted irradiation to measure the response of photovoltaic panels is a radiant intensity of 1000 W/m² and a temperature of 25°C

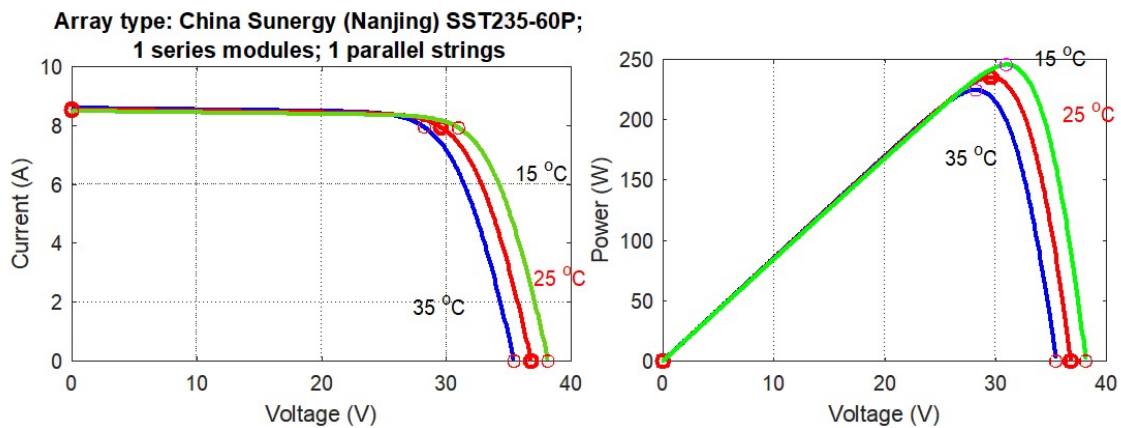


Fig III.9 Curve of variation of currant and power as a function of time

Table III.3 PV module parameter

Symbol	Values	Symbol	Values	Symbol	Values
P_{max} (W)	235.024	I_i(A)	8.5548	N_{cell}(A)	60
V_{co} (V)	36.8	I₀(A)	4.0556.10 ⁻¹⁰	I_{sc}(A)	8.54
V_{mp}	29.6	R_{sh}(ohms)	194.4803	I_{mp}(A)	7.94
T(V_{oc}) (%/deg.c)	-0.37	R_s(ohms)	0.33595	T(I_{sc}) (%/deg.c)	0.06

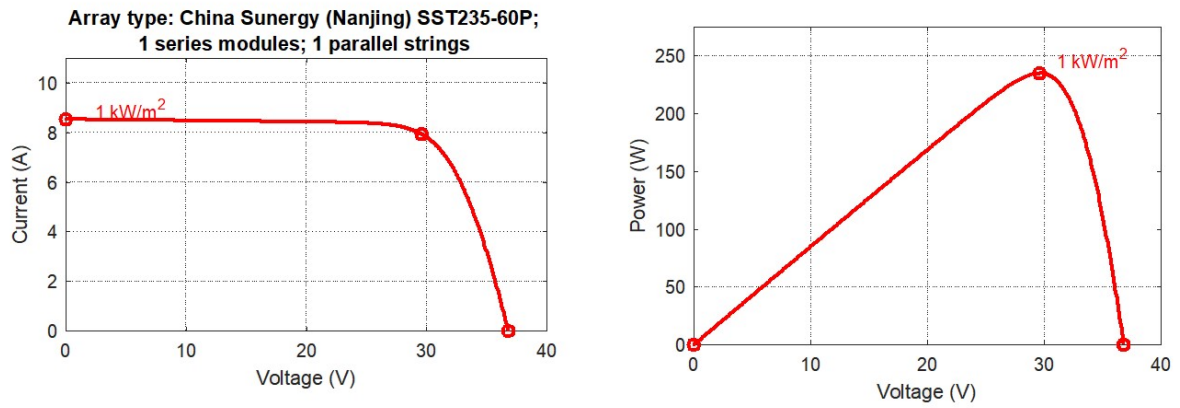
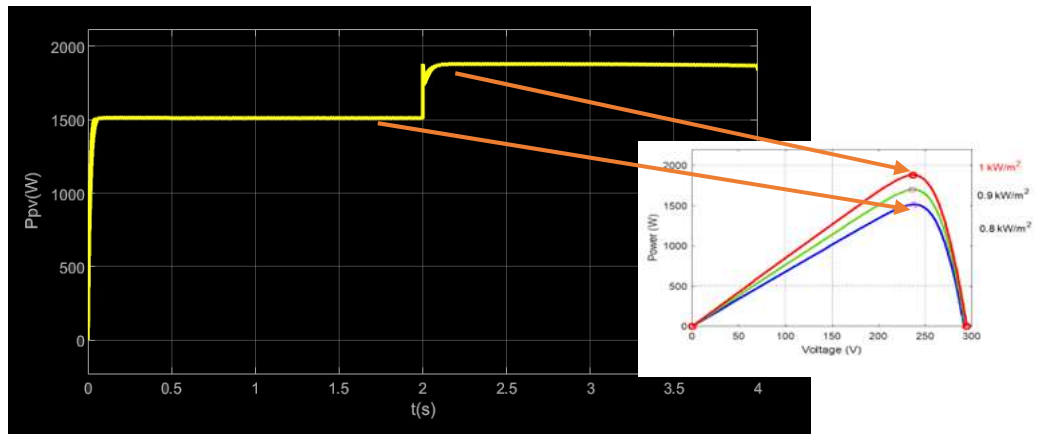


Fig III.11 Curve of variation of currant and power as a function of time



III.12 Curve of variation of hydrolic power as a function of time

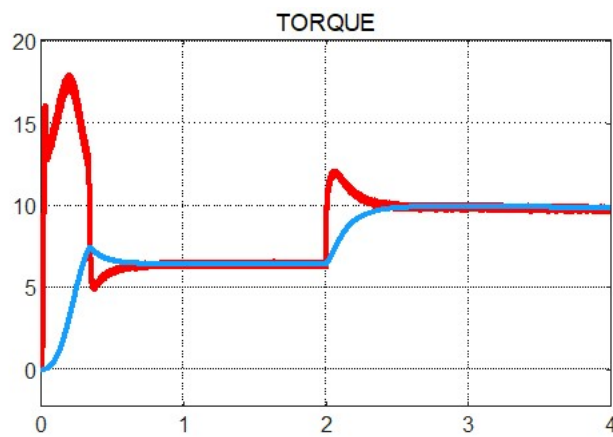


Fig III.13 Curve of variation of torque as a function of time

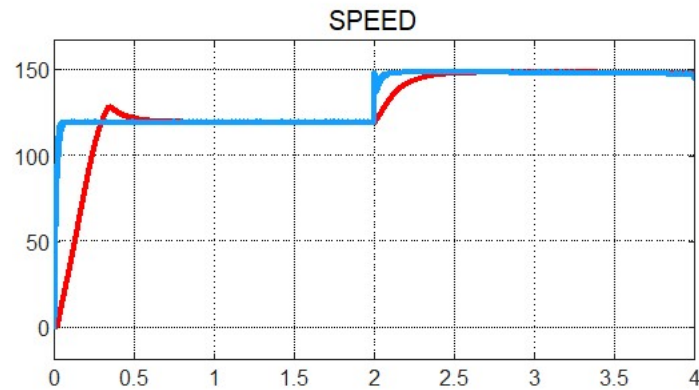


Fig III.14 Curve of variation of speed as a function of time

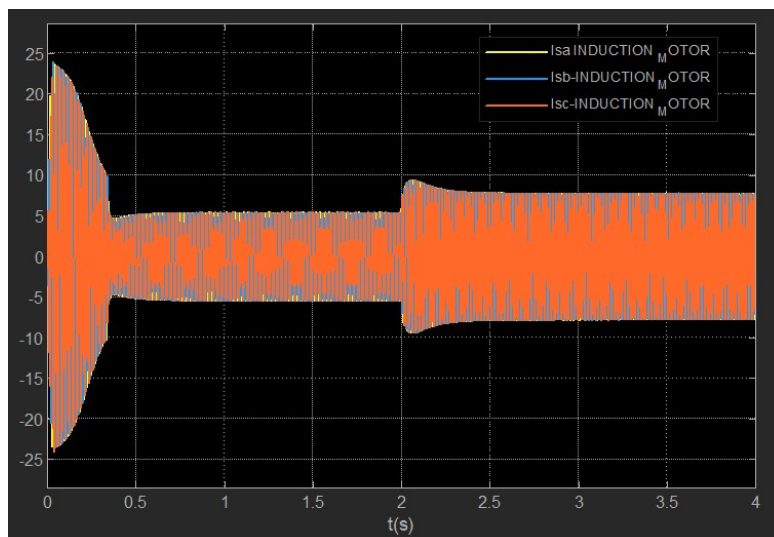


Fig III.15 Curve of variation of empty current as a function of time

III.6 Conclusion

In this chapter we have presented the sizing method of a photovoltaic pumping system, which allowed us to design a photovoltaic pumping plant to meet the water needs of a well-defined consumption and we developed under Matlab the simulation of the different photovoltaic pumping blocks. In this work, the performance of photovoltaic water pumping has been successfully improved on the basis of simulation studies under sudden changes in climatic conditions, and under the load variation the performance of the system using the DTC this command was analyzed which presented a command in closed loop we noticed that the system has less oscillations and behaved better during sudden changes of irradiation or charging.

General conclusion

Among the important advantages of photovoltaic conversion, the decentralization of energy production for small and widely dispersed communities, as already demonstrated by the solar pumps whose operation has proved to be very acceptable and the autonomy of the photovoltaic system, autonomy of place but equally important is operational autonomy. To avoid additional installation costs, most pumping systems photovoltaic function "above the sun" where the asynchronous motor coupled to the generator and a wave without energy storage. This arrangement is well suited for non-critical loads such as pumps, which do not require continuous operation throughout the day. Our work is focused on the modelling and control of a photovoltaic pumping system. The proposed system consists of a photovoltaic generator controlled by an MPPT algorithm to obtain the maximum power point, a static converter and a motor pump group. The converter is the boost chopper which is used to convert a DC voltage into another DC voltage of higher value, to power the motor pump group. In the first chapter we presented the photovoltaic system, and a reminder on the different combinations of photovoltaic systems, as well as their main components. In the second chapter we are interested in the modelling of all the elements of our photovoltaic pumping chain, each modelling is based on equations from the scientific literature. The third chapter was divided into two parts, in the first part we presented all the steps to follow for the proper sizing of the photovoltaic pumping system studied and we presented the DTC command method that we chose because of the simplicity of its implementation and the purpose of its use is to obtain an efficient dynamic control of the torque the results obtained from the simulation of our system studies under the environment MATLAB/ SIMULINK, and in the second part of this chapter we presented the MPPT method «Perturbations et Observation». The results, presented in this thesis, show that the use of this control allows to improve the efficiency of the photovoltaic pumping installation. Based on the results obtained and the use of the MPPT algorithm and the DTC control we can conclude that the photovoltaic water pumping performance has been successfully improved and the system has a remarkable energy autonomy and robustness against the sudden changes in load or sudden changes in load or sudden changes in climatic conditions. Based on the results obtained and the use of the MPPT algorithm and the DTC control we can conclude that the photovoltaic water pumping performance has been successfully improved and the system has a remarkable energy autonomy and robustness against the sudden changes in load or sudden changes in climatic conditions

BIBLIOGRAPHIQUES :

- [1] : F.Bendioudi et F.Lakhdari, « étude et simulation d'un système de pompage photovoltaïque avec batteries » ; Mémoire De Master, Université Abderrahmane Mira, Bejaïa, 2014.
- [2] : A. Belhocine et S.Zaidi, « étude et dimensionnement d'un système de pompage photovoltaïque autonome » ; Mémoire De Master., Université De Bejaïa, 2012.
- [3] : A. Ferrai, « Dimensionnement des Infrastructures Utilisant Diverses Sources Énergétiques Renouvelables Potentielles pour l'Alimentation Electrique d'un Village » ; Mémoire de magister, Ecole Nationale Polytechnique, Alger, 2008.
- [4] : J. ROYER, T. DJIAKO, E. SCHILLER et B. SADASY « Le pompage photovoltaïque» manuel de cours à l' intention des ingénieurs et des techniciens, IEPF, université d'Ottawa, EIER, CREPA.ISBN 2-89481-006-7, 1998.
- [5] : I.Bchsaiset A.Sebbagh A, « Optimisation d'un système de pompage photovoltaïque pour l'irrigation d'un hectare de palmier dattier en utilisant les méthodes métaheuristiques. » ; Mémoire de master, Université m'hamed Bougara-Boumerdes, 2017.
- [6] : A. Labouret, M. Viloz, « Energie solaire photovoltaïque », Le manuel du professionnel, Edition DUNOD, Paris - France, Août 2003.
- [7] : M.Benaïssa, « contribution a l'étude du transfert d'énergie dans les systèmes photovoltaïques » ; Thèse Doctorat, Université Djillali Liabes De Sidi-Bel-Abbès, 2018.
- [8] : L.Debbou et D.Maghribi, «commande d'un système hybride (photovoltaïque-éolienne) De production d'énergie» ; Mémoire D'ingénieur D'état. Université de Bejaïa, 2008.
- [9] : Belguelil Nadjat, « étude comparative du point de vue fonctionnement et maintenance des installations de pompes », mémoire de master, Université Mohamed Boudiaf M'sila, 2015.
- [10] : Jimmy Royer, thomas Djiako, Erico SCHILLER, Bokar Sada : «le pompage photovoltaïque».manuel de cour à l'intension des ingénieurs et des techniciens
- [11] : S.Zahar et C.Makhlouf, «etude et simulation d'un generateur photovoltaïque muni d'un convertisseur mppt pour une meilleur gestion energetique » ; Memoire De Master,Universite Mohamed Boudiaf – Msila, 2017.
- [12] : O.AMRANI, D.REKIOUA : « Etude et identification des différents modèles électriques photovoltaïques ». Université de Bejaïa.
- [13] : M.Abdelghani Bessem « Modélisation et simulation d'un pompage photovoltaïque » Université BADJI MOKHTAR-ANNABA ,2018.
- [14] : A. Hadj Arab, M. Benghanem et A. Gharbi, «Dimensionnement de Systèmes de Pompage Photovoltaïque» ; Revue des Énergies Renouvelables. Vol.8, pp (19 – 26), 2005.

Bibliographiques

- [15] : K. EL-Melouani, « dimensionnement d'un hacheur survolteur » ; Application noté de polytech Clermont-Ferrand, France, 2010.
- [16] :chahraze e, ai t .kahi na : « dimensionnement et installa on d' un système photovoltaïque ,applica on a la F .G. E. I ». Mé mo i re d' ingéni eur d' état en électronique université de T.O 2008-2009.
- [17] : D.Kefsi, F.Ouikene : « Commande d'un système de pompage photovoltaïque ». Mémoire d'ingénieur d'état en électrotechnique université de T.O 2009-2010.
- [18] : A.Hamidat,A.hadj Arab,F.chenlo and M.Abella « performances of the centrifugal and displacement pumps ».WREC1998,pp1951-1954
- [19] Carlos Canudas de Wit « Modélisation contrôle vectoriel et DTC » 2000
- [20] Bernard de Fornel « Techniques de l'ingénieur » D3 623
- [21] A. Ameer « commande sans capteur de vitesse par DTC d'une machine synchrone à aimants permanents dotée d'un observateur d'ordre complet à mode glissants » université de Batna 2005
- [23] M.G. Jayne « New Direct torque Control scheme » EPE 2005
- [24] : Mohamed Lakhdar Louazene, mémoire de magister, électrotechnique, option maîtrise d'énergie, Université El hadj lakhdar – batna, 2008. [26] : A. Bouden : « Analyse optimisée de système de pompage photovoltaïque». Mémoire de Magister en Electronique, Option : Instrumentation- Composants Electroniques et Systèmes 2008